INFORMATION TO USERS

This manuscript has been reproduced from the microfilm master. UMI films the text directly from the original or copy submitted. Thus, some thesis and dissertation copies are in typewriter face, while others may be from any type of computer printer.

The quality of this reproduction is dependent upon the quality of the copy submitted. Broken or indistinct print, colored or poor quality illustrations and photographs, print bleedthrough, substandard margins, and improper alignment can adversely affect reproduction.

In the unlikely event that the author did not send UMI a complete manuscript and there are missing pages, these will be noted. Also, if unauthorized copyright material had to be removed, a note will indicate the deletion.

Oversize materials (e.g., maps, drawings, charts) are reproduced by sectioning the original, beginning at the upper left-hand corner and continuing from left to right in equal sections with small overlaps. Each original is also photographed in one exposure and is included in reduced form at the back of the book.

Photographs included in the original manuscript have been reproduced xerographically in this copy. Higher quality 6" x 9" black and white photographic prints are available for any photographs or illustrations appearing in this copy for an additional charge. Contact UMI directly to order.

UMI

A prosthetic hand with tactile sensing

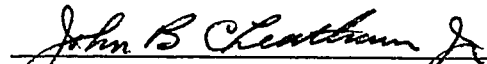Gunawardana, Ruvinda Vipul, M.S.

Rice University, 1994

RICE UNIVERSITY

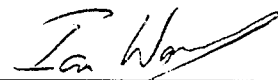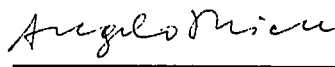# A PROSTHETIC HAND WITH TACTILE SENSING

by

RUVINDA V. GUNAWARDANA
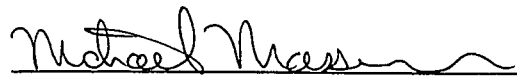
A THESIS SUBMITTED
IN PARTIAL FULFILLMENT OF THE
REQUIREMENTS FOR THE DEGREE OF
MASTER OF SCIENCE

APPROVED, THESIS COMMITTEE

Dr. John B. Cheatham Jr., Chairman
Professor of Mechanical Engineering

Dr. Ian D. Walker
Assistant Professor in Electrical
and Computer Engineering

Dr. Angelo Miele
A.J. Foyt Family Professor in Engineering
and Professor of Aerospace Sciences
and Mathematical Sciences

Dr. Michael J. Massimino
Adjunct Assistant Professor in the
Department of Mechanical Engineering

Houston, Texas
April, 1994

ABSTRACT

A PROSTHETIC HAND WITH TACTILE SENSING

by

Ruvinda V. Gunawardana

With recent advances in myoelectric signal processing, powered prosthetic hands with myoelectric control have become more accepted among users of prosthetic hands. Inspite of this progress, the hands that are currently available have limited functionality and provide little or no sensory feedback to the user. Thus the user cannot control the forces exerted by the hand on an object being grasped. The objective of the myoelectric hand project at Rice University is to create a hand that has greater functionality and also the ability to sense and control the forces. In the research described in this thesis, a prosthetic hand that is capable of controlling the grasp strength is built. Force Sensitive Resistors manufactured by Interlink electronics are used to sense the forces. These sensors are installed at eleven likely locations of contact. The system demonstrated the ability to control the grasp forces.

ACKNOWLEDGMENTS

TABLE OF CONTENTS

FIGURES

CHAPTER 1: INTRODUCTION

Over the years, prosthetic limbs have ranged from the wooden legs and hooked hands of the centuries past to the modern powered upper and lower limb prostheses of today (Hortensius, 1987). The use of electrical energy as a power source in a prosthetic hand was first reported in 1919 when Bochard invented an Electromagnetically powered hand (Bochard, 1919). This device and other early powered prosthetic hands lacked proper control and were not acceptable to prosthetic hand users. The use of electrical energy in a prosthesis did not gain importance until it was combined with myoelectric control (Näder, 1990). In the 1960s a considerable amount of progress was made in myoelectric control and a prosthetic hand using myoelectric control was produced commercially by Otto Bock company of Germany (Näder, 1990). Today there are many myoelectric control systems commercially available.

Even though a considerable amount of progress has been made in myoelectric control, the hands that are currently available provide little or no sensory feedback to the user. The human hand is an important source of sensory input and much of the sensory input and the proprioceptive feedback are lost in the amputation. Designers of myoelectric prosthesis have been singularly unsuccessful in the restoration of sensory feedback (Scott and Parker, 1988). The research described in this thesis is concerned

with the restoration of sensory information to the user of prosthetic devices.

1.1 THE OBJECTIVE OF THIS PROJECT:

The human arm presents an example of a structure that is capable of both delicate tactile sensing and precisely adjusted, coordinated movements (Moss-Salentijn, 1992). The hand is capable of providing tactile information (force and location) with very high spatial resolution which enables humans to detect the shape and orientation of objects using tactile information only. The hand is also capable of detecting slip, heat, cold and a human can also sense the orientation of the arm joints.

Out of this information, even though detecting the presence of extreme heat or extreme cold could be useful for the protection of the prosthesis and also for the user in certain situations, the inability to detect temperature is not as serious a problem as the inability to detect grasp force or slip to the amputee. The orientation of the arm and finger joints can be detected using suitable position sensors and this is already done with prosthetic and robotic devices. Therefore, providing tactile information to the user and providing the ability to detect slip are the two areas that are of most value and interest to prosthetic hand users.

The popular approach taken by most researchers, is to provide all of the sensory information to the user and to make the user control the hand (Kato, 1969), (Giampapa 1989), (Scott, 1980). The problem with this method is that it requires efficient and fast communication between the arm and the user in both directions (from the user to the arm and from the sensors to the user) and the channels of communication available are limited.

The popularly used channel of communication from the user to the hand is through the myoelectric signals and the amount of information that can be transmitted through this channel is limited and would not be sufficient to control a complex arm effectively. The devices used to convey the sensory information to the user are called display devices (these will be discussed in greater detail in chapter 2) and the amount of information that can be conveyed through the display devices is also limited and also these cause a delay in response time which could be disastrous.

For these reasons an alternative approach taken by some researchers is to have a computer on board the arm which performs some processing and control (Hortensius, 1987). This is the approach taken by the researchers at Rice University. In our project, the on board computer will receive high level commands from the user through the myoelectric signals and then perform local control of the arm using the sensory information from the sensors. It will also perform some local processing of the sensory information and then convey the processed information back to the user through a display

device. The designing of the display device is beyond the scope of this project. Therefore we concentrated on building a hand and a system of sensors and interfacing these to a computer. The system would be compatible with display devices designed by other researchers. Slip detection was also beyond the scope of this project.

1.2 STATEMENT OF PURPOSE:

The objective of the research described in this project is to design and construct a prosthetic hand that is capable of using the information provided by the myoelectric signal processor and implement a grasp based on the users intent. For this purpose, we will assume that the myoelectric signal processor can determine the level of grasp force (one of three levels: soft, medium or hard) and also the type of grasp from one of the following grasps.

1. Key grasp
2. Briefcase grasp
3. Three point chuck
4. Cylindrical

The system should be able to achieve the desired grasp and to maintain the desired force level at the hand/object interface. The system consists of the hand including potentiometers and force sensors, the computer, the circuit that controls the motor and the circuit that interfaces the sensors to the computer.

1.3 ORGANIZATION OF THE TEXT:

After this introductory chapter, a more detailed description of the different components of the myoelectric hand project will be presented in chapter two. A description of the components of the system built for this project is given in chapter three. In chapter four, the selection process of a suitable tactile sensor, and a description of the selected sensor and its calibration are discussed.

The dynamics and control of the hand and the estimates of friction are described in chapter five. The algorithm that implements the control law and experimental results are presented in chapter six. This thesis concludes in chapter seven with a summary of this project and some suggestions for future extensions.

CHAPTER 2: THE COMPONENTS OF THE MYOELECTRIC HAND PROJECT

2.1 INTRODUCTION:

At present most commercially available prosthetic hands can typically achieve only one grip since they have only one degree of freedom. This creates a considerable limitation to the kinds of objects that can be grasped. In addition, due to lack of sensors (other than position sensors) the user cannot control the grasp force, and also due to lack force feedback to the user, he/she is deprived of the sensory information that a normally able person gets from the hand.

The objective of the prosthetic hand research project at Rice University is to solve some of these problems. In order to achieve this, several components of the overall prosthetic hand need to be improved. The first step is to increase the functionality of the prosthetic hand. This task has been assigned to a group of Senior Mechanical Engineering students. The current design that the students are working on is likely to be able to achieve several grips. These include the chuck, cylindrical , key and briefcase grips (Baker, 1993).

In order to achieve our goals we need much more sophisticated communication, sensing and control systems. The

overall system that we would like to design can be represented in block
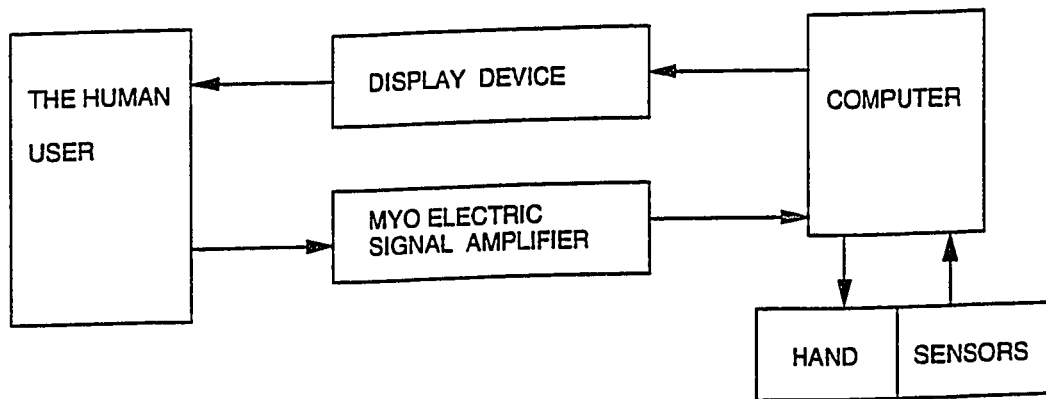
FIGURE 2.1: The components of the myoelectric hand

diagram form (Figure 2.1). The system consists of the user, the electrodes and the amplifier circuit for the myoelectric signal processing, a single board computer, the prosthetic hand, the sensors and a suitable display device to provide the user with some of the sensory information. The myoelectric signals generated by the user are amplified and fed to the computer which will interpret from these, the intentions of the user. Based on the users needs the computer will then implement a control loop that will implement the desired action.

In addition to this, it is also highly desirable for the user to be provided with some of the sensory information. In this system we

hope to first process the sensory information received from the sensors and then display to the user the processed information which will be much easier for the user to interpret.

In the rest of this chapter, the myoelectric signal processing and the justification for the computer will be discussed. Next, the sensors will be discussed and finally methods of displaying the sensory information to the user will be considered. The research for this thesis, concentrates mainly on the installation of sensors in a prosthetic hand and the implementation of a control law that will achieve the objectives of the user.

2.2 MYOELECTRIC CONTROL:

Myoelectric control uses the electric activity of a contracting muscle as a control signal (Scott, 1988). In a myoelectric prosthesis, muscle remnants in the residual limb are used to provide control signals for powered components. The first published account of myoelectric control was by Reiter in 1948 (Reiter, 1948). But this work was not followed up and it wasn't until the 1960's that myoelectric control became clinically significant. Currently, myoelectrically controlled prosthetic hands have become more popular and they have been fitted successfully to a large number of amputees world wide (Näder, 1990). In the prosthetic hand project at Rice University, the objective of the researchers working on myoelectric signal processing is to identify different grasps by using

multiple channels of myoelectric signals (Farry,1993). Each channel has two electrodes.

An electrode placed on the skin surface can measure the passing of action potentials propagating along muscle fibers underneath the electrodes as the fibers contract. The electrodes measure the sum of all action potentials. Researchers in the early 1970's treated the myoelectric signal as amplitude modulated signals whose amplitude is proportional to the force developed by the muscles. By the late 70's the model had matured to treat the signal as amplitude modulated Gaussian noise whose variance is proportional to the force (Farry, 1993). In recent years, researchers have successfully refined force estimations from the myoelectric signals.

Other researchers have considered shape and spectral characteristics of the myoelectric signal. The approach taken by Kristin Farry, a Doctoral student in the Electrical Engineering department of Rice University is to use the myoelectric spectrum (over a range of frequencies) of multiple channels to discriminate between different grasps.

2.3 THE COMPUTER

The one degree of freedom prostheses currently available do not require a computer. In these, the myoelectric signal can be made to directly open or close the single joint. However, in the case of a multiple degree of freedom hand capable of achieving multiple grasps, if we make each of the myoelectric channels control each joint it would require a tremendous amount of concentration from the user to achieve a given grasp. This would probably make the hand very unpopular and would lead to rejection. In order to make the prosthesis attractive to the user, the system should be intuitive and easy to control. The best method to achieve this would be to have the system capable of processing the myoelectric signals from the user and identifying the desired grasp and then implementing a control algorithm that will achieve the desired grasp. All of this can only be achieved by having a single board computer inside the prosthetic arm.

2.4 SENSORS:

A common criticism of externally powered artificial limbs is that the user is deprived of the (limited) feedback that would have been provided by the harness of a body powered prosthesis (Scott, 1980). This criticism is valid and it helps focus our attention to the need for sensory feedback in an externally powered prosthetic hand.

Most currently available commercial prosthetic hands have few or no sensors other than those used to read the positions of joints. As a result all of the information that a normally able person gets from his/her hand is not available to the user of a prosthetic hand (Scott and Parker, 1988). Among this information, the grip force and the ability to detect slip are two of the most important pieces of information that are missing.

The fact that a prosthetic hand user does not have the ability to detect the grip force makes it difficult or impossible for the user to control the grip force. As a result it would be impossible to pick up a delicate object like an egg without crushing it. It would also be difficult to grip a heavy object without dropping it. The lack of ability to detect and control the grip force limits the use of current prosthetic hands.

The inability to detect slip when holding an object places an extra burden on the user of a prosthetic hand. In order to prevent the object being held from falling, the prosthetic hand user needs to apply a large force and thereby waste energy. More importantly there can be situations where it is not practical to apply a large grip force (if the object is delicate). In this case the user may have to rely on his vision to ensure that the object does not slip. This would however, seriously limit the practical utility of the hand.

The purpose of this research is to reduce the limitations in the use of prosthetic hands, caused by the lack of sensory information

that a normally able person gets from the hand. In this section, some of the past work in this area will be reviewed.

2.4.1 Tactile Sensing in Prosthetic Hands - State of the Art:

The need for tactile sensing in prosthetic devices has been recognized by researchers for some time (Scott, 1988) and several prosthetic hands with tactile sensing capability have been developed. A prosthetic hand developed by a study group centered around Kato had pressure sensors attached to the fingertip and the fingertip pressure was fed back to the user by a mechanical vibrator attached to the skin. The amplitude of the 100 Hz sine waves generated by the mechanical vibrator was made proportional to the pressure (Kato, 1969).

Giampapa, has presented a number of requirements that a sensor system that can be installed in a prosthetic hand should meet (Giampapa, 1989).

1. The device should be simple in design and maintenance.

2. It should be light weight.

3. It should be small enough to fit as a self contained unit in a prosthetic hand.

4. The unit should be simple enough to permit the patient to master it.

5. The sensation transmitted to the patient should be easily identifiable & distinguishable from other sensory stimuli.

He has described a sensory system that consists of force sensors that are located at the fingertips. When these sensors detect force, the information is conveyed to the user by means of a vibratory transducer that produces a vibration of selected frequency for each unit. (The hand is divided into three units) The intensity of the vibration is used to indicate the magnitude of the force while the frequency is used to indicate location. The intensity is proportional to the force.

Scott, et al. (1980) designed a force sensor system that consists of simple strain gauges which measure the bending moment in the index finger of the artificial hand. This system uses electric stimulation of the skin as a means of communication to the user. The stimulation rate is proportional to the pinch force. A stimulation rate of 0 to 60 pulses per second correspond to pinch forces from 0 to 100 N (Scott, 1980).

2.4.2 Slip Detection in Prosthetic Hands - State of the Art:

The importance of slip detection for prosthetic hands has been recognized by several researchers in the past (Knox, 1992), (Winkler, 1992), (Kyberd,1992). Slip detection was used in an artificial reflex system implemented by Knox, Childress and Heckathorne (Knox, 92). In this system, the prehension force in an artificial hand or robotic gripper where this system is implemented, is increased when slip is detected. The artificial reflex implemented here, is a feedback loop that bypasses the human operator and operates directly through the control system of the device. This eliminates human response delays associated with supplemental sensory inputs and provides an overall quicker response to slip. In this system the user initiates the grasp of an object and the prehensor attempts to maintain it.

The slip detector used in the artificial reflex system detects the vibrations caused by a slipping object. The main design challenge faced by the designers was to eliminate other unwanted noise (vibrations). These included noise caused by the motor while closing the gripper and noise due to incidental contact of the prosthesis with other objects.

Two methods have been used to detect slip. The first method is to create a sensor that can detect the vibrations caused by the slipping object. In the second method a tactile sensor with relatively high resolution and an algorithm that can detect the shift in the

pattern of forces caused by the movement of the slipping object is used (Chappel, 1991).

Kyberd and Chappel (Kyberd,1992), constructed a sensor that is capable of detecting both the contact force and slip, based on an optical beam and an acoustic slip sensor. It was used successfully in a range of artificial hands. The force response was nonlinear but repeatable. The design insured good response to vibrations caused by slip and poor response to vibrations caused by other disturbances. This was achieved by creating a system with a resonance frequency in the range of the frequencies of vibrations caused by slipping objects.

One of the problems with the second method of detecting slip (by using a tactile sensor and the shift in the pattern of forces) is the need to have a large number of force sensors to achieve high spatial resolution. However, it may be possible use this method to get a less reliable estimate of slip with a smaller number of sensors. Kyberd and Chappel, suggested using a combination of both methods of slip detection to get a better estimate of slip (Kyberd, 1992).

2.5 USER FEEDBACK:

It is highly desirable for the user of a prosthetic hand to be able to regain some of the sensory information that has been lost. In this case we would like to have a method of displaying the grasp force to the user. A device that uses some other channel of sensory input to the brain can be used for this purpose. Some of the more common modes of displays in prosthetic devices and in sensory substitution systems are,

(1) Vibrotactile and Electrotactile

(2) Audio

(3) Visual

In addition to these, devices that apply pressure on the skin in some other part of the body have also been used.

2.5.1 Vibrotactile and Electrotactile Displays:

The most commonly used devices for displaying force information in prosthetic research have been vibrotactile and electrotactile devices (Scott, 1988), (Kato,1969) and (Giampapa, 1989). Vibrotactile devices evoke tactile sensations using mechanical vibrations of the skin, typically at frequencies of 10-500 Hz (Kaczmarek, 1991). In electrotactile stimulation a tactile sensation is evoked by passing a local electric current through the

skin. The ability to vary the frequency and amplitude independently provide two channels of display for each electrode.

In addition to prosthetic devices, electrotactile and vibrotactile devices have been used in sensory substitution systems for many applications. Massimino studied the capabilities of a sensory substitution system for force feedback in teleoperation (Massimino, 1992). This system consisted of both vibrotactile and auditory feedback. Leder et al., used a vibrotactile display in an auditory prosthesis where the vibration intensity was increased with increase in sound intensity as sensed by a microphone (Leder, 1986).

Some of the potential drawbacks to using vibrotactile and electrotactile displays for this application are, irritations caused by the continuous action of the electrodes, the possibility of causing skin burns and the need to wear the display device at all times. (The vibrator has to be attached in a manner that the user can feel the sensations and this could make the device uncomfortable particularly in hot, humid weather)

2.5.2 Audio Displays

Due to the active role played by vision in our daily lives, the powerful abilities of our auditory system may go unnoticed. Our reaction time is faster to a sound stimulus than to a visual signal(Welch 1986).

Auditory displays have been used extensively to provide information to aircraft pilots. DeFlorez conducted a series of experiments that established aural reference axes that could be substituted for visual ones during instrument flying conditions (deFlorez, 1986). Auditory displays have been used to enhance other displays for aircraft pilots. In addition, audio displays have been used as computer interfaces, and also in guidance systems for blind people.

In this project, audio displays can be used as an alternative to tactile or visual displays. One of the key points to bear in mind in designing an auditory display for a prosthetic arm, is that it should not interfere with other important sounds. This is an area that needs further investigation.

2.5.3 Visual Displays:

Visual displays use the peripheral vision of the user to display information. Dr. Thomas Krouskop at The Institute for Rehabilitation

Research (TIRR) is working on an audio display that can be attached to a pair of spectacles or sun glasses (Krouskop, 1994). This device consists of a line of thin Light Emitting Diodes. In this, the color and the number of L.E.D.s can be used to provide two channels of information to the user. This device can be attractive to the user as it would not require the user to wear an additional device.

Any one of vibrotactile, electrotactile, audio or visual displays can be used in the prosthetic hand in our project. It is hoped that at some future time it will be possible to give the user the option to select the device that he/she feels most comfortable with, out of any one of these. It is important to note that the amount of information that can be displayed to the user is limited. (A large amount of information would require too much concentration by the user and would lead to its rejection). For this reason, it would be best to convey the sensed information to the computer and then have the computer process these data and convey to the display device information that is easy for the user to interpret.

2.6 SUMMARY:

The objective of the prosthetic hand research project at Rice University is to solve some of the limitations to the use of currently available prosthetic hands due to the limited functionality and lack of sensors. In order to achieve this, several components of the over all project must be improved. A group of senior mechanical

engineering students are working towards improving the functionality of the hand. Other graduate students are working on myoelectric signal processing. The work done for this thesis is involved with the creation of a system that is capable of achieving a grasp that the user desires based on tactile sensory feedback.

CHAPTER 3: THE COMPONENTS OF THE HAND BUILT FOR THIS RESEARCH

3.1 INTRODUCTION:

The system built for the research described in this thesis consists of the hand, the tactile sensors, the potentiometers and the circuitry used to interface the motors and the sensors to an IBM 386 P.C. Each of these components is described in this chapter. The tactile sensor is described in more detail in the next chapter.

3.2 THE HAND:

The hand which has been made to look similar to the human left hand contains four motors. The first three motors control the thumb, forefinger and the middle finger while the fourth motor controls the last two fingers which are coupled. Each finger molded of a high strength easily moldable epoxy resin has one degree of freedom. Each motor drives a power screw which is connected by a link to a finger. The body is made of aluminum.

3.3 THE POTENTIOMETERS:

Each finger has been equipped with potentiometers to measure the linear distance the power screw (nut) travels. The relationship between this distance and the finger joint angle is known so the potentiometer enables the computer to know the orientation of the finger at all times. The 50 K.ohm potentiometers are connected through a simple circuit to the computer.

For the potentiometers we require a circuit that converts the variable resistance in the potentiometers to a voltage that is proportional to it. We used a simple voltage divider circuit and an amplifier to isolate the input from the output (figure 3.1). The relationship between the output voltage and the resistance is given by,

$$V_{out} = \frac{R_{POT}}{(50K + R_C)} \left(\frac{R_1 + R_2}{R_2} \right)$$

Since the terms in the bracket and in the denominator are constant, the voltage is proportional to R_{pot}. The outputs are connected to the A/D converter. The resistors in the circuit were chosen such that V_{out} would be in the desired range for the A/D converter.
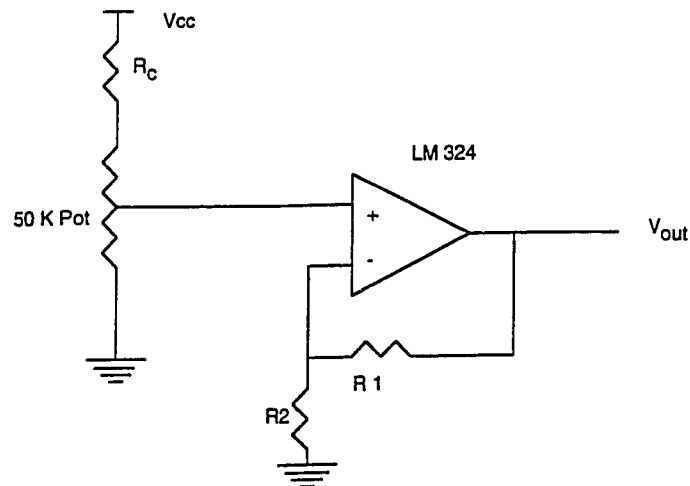
FIGURE 3.1 The circuit used for the potentiometers.

3.4 THE TACTILE SENSOR:

The purpose of a tactile sensor is to detect the contact forces that the hand is applying on any object that it is holding. To do this reliably the sensors must cover all of the area that an object might contact. However, due to the wide range of objects that may be held by the hand, this necessitates covering a large area with sensors.

Due to space, weight and power constraints in prosthetic devices the number of sensors that can be installed in the hand is limited. Having a smaller number of sensors covering a large area would seriously reduce the spatial resolution of the system and we

would like to have a relatively high spatial resolution. The reason for this is, in addition to the force we would like also to know the location of the force as the moment at the joint depends on both the force and the location of the force. Thus the sensor that we need can be considered a tactile sensor.
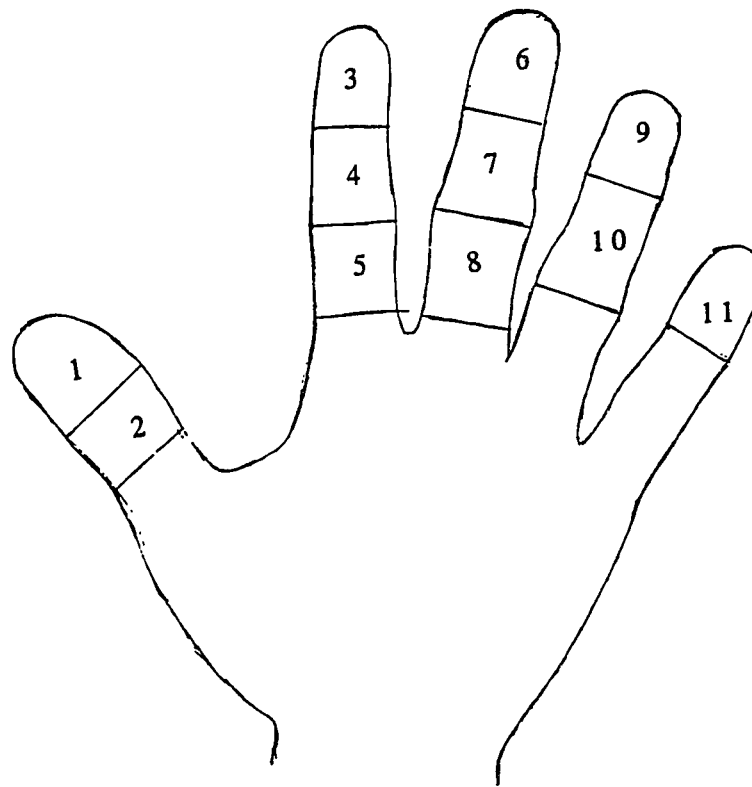
FIGURE 3.2: The Location Of Force Sensors In The Hand

Due to all of these reasons we have had to compromise on each of these design parameters (the area covered, the spatial resolution and the number of sensors). In this project we chose to install 11

force sensors on the hand. The force sensors do not cover the entire hand, but cover most of the likely locations of contact (Figure 3.2).

3.5 THE A/D CONVERTERS

The output from the sensors are analog and each of these outputs needs to be presented in a digital format to the computer. We used the ADC 0809 A/D (Analog to Digital) converter chip manufactured by JDR Microdevices as our A/D converter. This chip has eight analog input channels and gives an eight bit digital representation of the input which results in a range of (0-255). It requires 100 microseconds to complete one conversion and the channel to be converted is selected by three address lines. We installed three of these chips which will allow us to interface up to 24 analog inputs. The data sheet for the ADC 0809 chip has been included in appendix B.

3.6 THE MOTOR CIRCUIT:

It is desirable for this system to be able to control the voltage in to the motors and so the circuit was designed to provide 16 levels of voltage. It is also necessary to be able to reverse the direction of the motor rotation. For the motors that were used, (DC MicroMo® series 1219 and 1331) the direction can be reversed by changing the polarity of the input voltage.

The circuit implements pulse width modulation using a binary counter. The desired voltage level is down loaded to a counter which is configured to count down to zero and stop. Outputs from the counter are connected to an OR gate. As a result, the output from the OR gate remains high as long as the counter is counting and becomes zero when it stops. Thus, the output from the OR gate has a pulse width proportional to the desired voltage. The counters are loaded with the desired voltage level at a frequency that is 1/16 that of the clock in the counters.

A switching circuit consisting of four Field Effect Transistors is used to change the direction of the motor rotation.

3.7 SUMMARY:

The components of the hand built for this project are described in this chapter. The hand containing four motors has been designed to look similar to the human left hand. Four 50 K Ohm potentiometers are used to measure the joint angles. The hand has 11 tactile sensors located at locations that are likely to be in contact with grasped objects. The sensors are connected to the computer using three A/D converters each with 8 channels providing a total of 24 analog channels. The motors are controlled with a circuit that implements pulse width modulation allowing for 16 levels of voltage to the motors in each direction of rotation.

CHAPTER 4: THE TACTILE SENSOR

4.1 INTRODUCTION:

The process of selecting a tactile sensor based on the specifications of our project is described in this chapter. The specifications are presented in section 4.2. This is followed by a description of different tactile sensor designs with an evaluation of each of them for this project. In section 4.4, the selected sensor is described followed by a description of the circuit used to interface the sensor to the computer and the calibration procedure.

4.2 THE SPECIFICATIONS FOR THE TACTILE SENSOR:

A survey of researchers and industrial manufacturers by Leon D. Harmon of Case Western Reserve University led to a set of general requirements for tactile sensors (Harmon, 1982). Even though some of these specifications are too strong for our application, it can be used as a general guideline.

(1) <u>The spatial resolution:</u> A spatial resolution of 1-2 mm. was suggested in the specifications by Harmon. However, due to limitations discussed in chapter 3, it is not practical to have a spatial resolution of 1-2 mm. For the present time we will be satisfied with a spatial resolution of 10 -20 mm.

(2) <u>Force Sensitivity:</u> The suggested force sensitivity is 0.5-10 grams. For our application, even though we would like to have very high force sensitivity we can manage with a sensitivity of 10-20 grams.

(3) <u>The dynamic range:</u> A dynamic range 1000:1 is desirable and often a logarithmic response is satisfactory. That is, for small forces high sensitivity is more important than it is for a large force.

(4) <u>Sensor Bandwidth:</u> The sensor bandwidth should extend from dc to at least 100 Hz. (The band width influences the overall frequency response of a control loop) However, since the frequency of the component of the human touch extend only up to 20 Hz this requirement can be relaxed somewhat.

(5) <u>Linearity:</u> Linearity is desirable, but some non linearity can be tolerated. As long as the sensor has good repeatability and stability, the non linearity can be compensated. In our application, we are looking for a range of force. For this reason we can tolerate non linearity.

(6) <u>Hysteresis:</u> Hysteresis must be low. That is the output should depend only on the input and not whether the input is increasing or decreasing.

(7) <u>Durability:</u> Sensors must be wear resistant, especially with slip. They must also be rugged to withstand harsh environments.

(8) <u>Power consumption:</u> Low power consumption is extremely important. If the sensor consumes too much power and leads to significantly decreased life of the batteries, it would lead to immediate rejection by the users.

(9) <u>Packaging:</u> The sensor and the processing circuitry must satisfy the space and weight constraints of a prosthetic hand.

Based on these requirements we set about selecting a suitable sensor for out application. The details of this decision will be presented next.

4.3 METHODS OF TRANSDUCTION:

Typically, tactile sensors convert force to an electronically measurable quantity. Tactile sensors can be classified based on their method of transduction. The following is a list of methods of transduction.

1. Optical
2. Piezoelectric and Pyroelectric
3. Capacitive
4. Magnetic

5. Strain gage

6. Resistive

After considering several sensors we decided to use Force Sensitive Resistors produced by Interlink Corporation (Interlink electronics, 1994). As implied by their name these sensors fall into the category of resistive tactile sensors.

4.3.1 Optical:

Optical tactile sensors can be designed to provide very high spatial resolution and high sensitivity how ever, they may have some hysteresis. An overview of these sensors and a detailed presentation of the theory can be found in the reference (Silvermintz, 1988). The optics based tactile sensors that are commercially available are generally larger (thicker) than Force Sensitive Resisters which would have made their installation much more involved for this application.

4.3.2 Piezoelectric and Pyroelectric:

The Piezoelectric effect is the generation of voltage across a sensing element when pressure is applied to it. The voltage generated is proportional to the applied pressure. (Nicholls, 1992) The pyroelectric effect is the generation of a voltage when the

sensing element is heated or cooled. The main disadvantage with these sensors is that their response is dynamic. That is, if the same force is maintained their output decays to zero. The second problem is, it is hard to distinguish piezoelectric effects from pyroelectric effects.

4.3.3 Capacitive:

Capacitive sensors are basically capacitors in which the capacity changes with applied force. Capacitive sensors offer a wide dynamic range and a linear response. The change in capacity can be converted a change in voltage or frequency using the appropriate circuit. The biggest drawback with capacitive sensors is that they are susceptible to noise and the stray capacitance introduced in the system can decrease the sensitivity of the sensor (Seow, 1988), (Nicholls, 1992).

4.3.4: Magnetic Transduction Methods:

Sensors using magnetic transduction can be divided in to two basic categories. The sensors in the first category use mechanical movement to produce a change in magnetic flux (Nicholls, 1992) (Figure 4.1). The second category uses magneto elastic materials which show a change in magnetic when subject to mechanical stress.
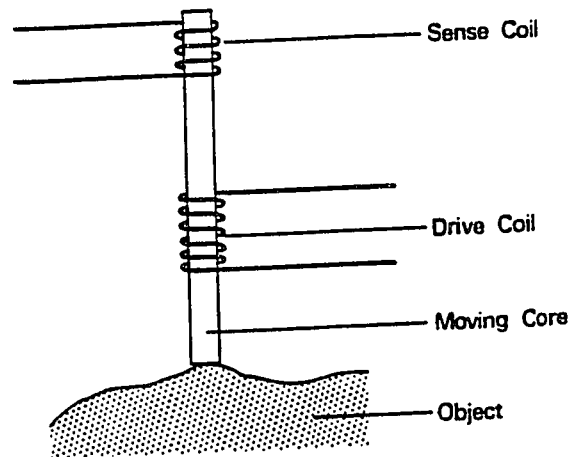
FIGURE 4.1: Magnetic Tactile Element

(Source: Nicholls, H.R. "Tactile Sensing Designs", <u>Advanced</u> <u>Tactile Sensing For Robotics</u> , Nicholls, H.R. Editor, World Scientific, Singapore 1992 p 26)

The force sensors belonging to the first category have a wide dynamic range and allows for large displacements however, they are bulky. The second category of sensors offer low hysteresis and linear response and also the capability to measure the shear force and torque in addition to the normal force. The problem with these sensors for this application is, they require an A. C. power source which is not available in our system.

4.3.5 Strain Gage:

Electrical strain gages are the best known and most widely used force transducers (Grisham, 1992). Even though they also use change in resistance as the method of transduction, they deserve special attention. Strain gages operate on the principle that an applied pressure (or stress) produces a mechanical deformation in a conductive material that gives rise to a change of resistance. Strain gages have been used on both the Stanford/JPL and the Utah/MIT hands. Semiconductor strain gages are attached to each cable (tendon) at the point where it enters the finger (Dario, 1986). Strain gages have also been successfully used in six component force/torque sensors.

The main drawback to using strain gages in this application is the difficulty in installing a strain gage within the space constraints of the finger such that the desired fingertip force can be measured reliably.

4.3.6 Resistive:

Of all the methods of transduction discussed in this chapter, the method that has received the most attention is concerned with sensors based on materials whose resistance change with applied force. Typically, these materials are carbon or silicon (or any conductive material) doped rubber called conductive rubber. In

typical resistive sensors, the conductive rubber, and the electrodes are configured such that more conductive particles come into contact with the electrodes and with each other as the applied force is increased resulting in a decrease in the resistance between the electrodes.

The advantages of using these sensors include durability, wide dynamic range, the simplicity of the circuitry needed to convert the change in force to a change in voltage and very importantly for this application, they are very thin and relatively small in size which makes it easy to install them in the fingers such that the desired forces can be measured. However, some of these sensors have a considerable amount of hysteresis and also the response is nonlinear.

4.4 THE INTERLINK FORCE SENSITIVE RESISTOR:

Out of all of the sensors considered, we felt that the Force Sensitive Resistors (F.S.R.) manufactured by Interlink Electronics are the most suitable for this application. These sensors are constructed by depositing a conductive pattern on one polymer in the form of an open interdigiting set of electrodes and a proprietary semiconductive polymer layer on the other polymer (Figure 4.2). When they are placed together, the electrodes are shunted to each other by the conductive polymer. With no pressure, the resistance reaches a
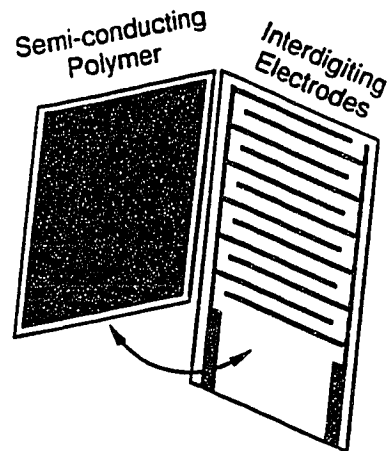
FIGURE 4.2: The F.S.R. Construction

(Source: Interlink Electronics, <u>Technical Overview</u>, "Electrical Interfacing" February, 1990.)
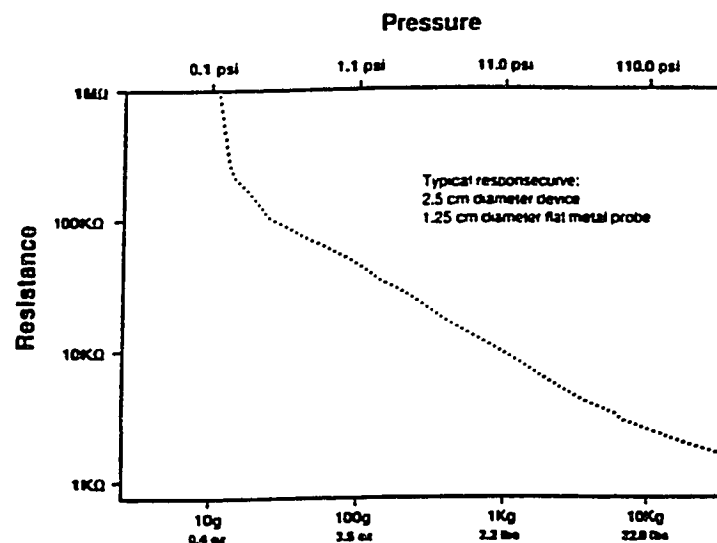
FIGURE 4.3 Force/Resistance Characteristic Curve

(Source: Interlink Electronics, <u>FSR</u> TM <u>Technical Specifications,</u> Rev 81151891, August 1989)

maximum (greater than 1 Mega Ohm for this sensor) (Interlink electronics, 90). The Force/ Resistance response is nonlinear (Figure 4.3). In our system, we are satisfied with the several discrete points and so the non linearity does not create any problem. The sensors are 0.2 inches in diameter and are 0.01 inches thick.

4.5 INSTALLATION:

Since the fingers were molded as one piece, the sensors were installed by cutting a small piece of the finger out and then attaching it back again to the finger with two screw after placing the F.S.R. on the flat surface in between (Figure 4.4) The screw hole was made
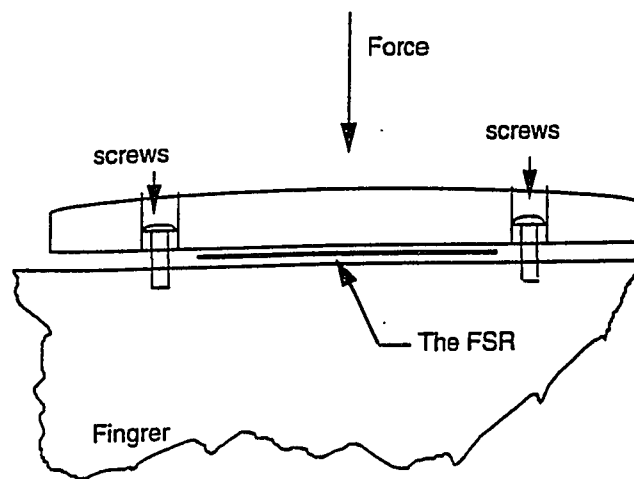
FIGURE 4.4: The installation of the Force Sensitive Resistor.

such that the piece is free to move in the direction of force. The screws merely prevented the piece from falling. This is important because if the screws interfere with the motion of the piece, they would cause the sensor to preload and lose its sensitivity.

4.6 THE FORCE SENSOR CIRCUIT:

The first step in reading the force sensors is to convert the variable resistance to a voltage. The circuit used for this purpose is the FSR voltage divider circuit presented in the Interlink Technical notes guide (Figure 4.5). By changing the resistance R_m the response
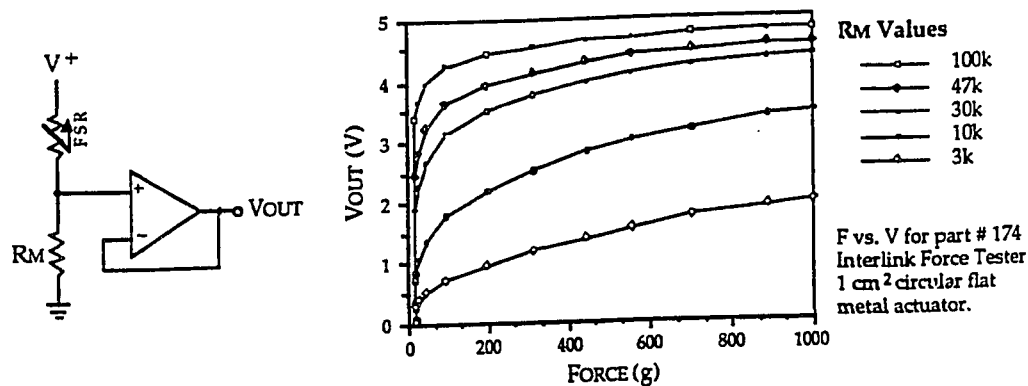
FIGURE 4.5: FSR Voltage divider

(Source: A Technote: Suggested Electrical Interfaces for Force Sensing Resistors[TM])

can be adjusted. We chose a resistance of 43 K Ohm as that gave the best response for the range of forces that was expected. As recommended, we chose the LM324 operational Amplifier manufactured by National Semiconductor.

4.7 SENSOR CALIBRATION:

Once the circuit for the sensors was completed and connected through the A/D converter to the computer, the next step was to calibrate them. For our algorithm, it was sufficient to calibrate a few discrete points rather than generating a continuous function relating the force to the voltage value in the computer since we are only interested in maintaining the forces within a range.

We chose force readings of 4, 8, 16 and 32 ounces for this application and each of the sensors were calibrated. The results have been presented in table 4.1. after converting the voltage readings in the computer (the eight bit representation between 0 and 255) to volts. It can be seen that the numbers vary considerably from sensor to sensor. This is partly due to the different levels of pre-loading of the sensors during installation. In addition, the response of the sensors themselves vary. After calibrating, these numbers were hard coded into the subroutine that reads the sensors.

Sensor number	Voltage at 4 oz. (volts)	Voltage at 8 oz. (volts)	Voltage at 1 lb. (volts)	Voltage at 2 lb. (volts)
1	0.69	0.82	1.02	2.21
2	1.50	2.23	2.43	2.61
3	0.27	0.30	0.59	1.91
4	1.16	1.61	2.47	3.13
5	0.59	0.99	1.55	2.75
6	0.81	2.25	2.82	3.33
7	1.86	2.35	2.92	3.37
8	1.37	2.02	2.47	2.95
9	0.46	0.61	0.73	1.55
10	1.07	2.25	2.82	3.18
11	0.52	0.55	0.64	1.46

TABLE 4.1: The Voltage read by the computer at different levels of force for the Force Sensitive Resistors.

4.8 SUMMARY:

In this chapter, the selection and the application of the force sensor was described. Based on the specifications we chose to use the Force Sensitive Resistor designed by Interlink Electronics. The sensors were installed by cutting a small piece off of the finger and placing the sensor in between finger and the piece which was reconnected by two screws. The sensor was calibrated at several discrete levels of force.

CHAPTER 5: DYNAMICS AND CONTROL

5.1 INTRODUCTION:

In this chapter the dynamics and the control of the prosthetic hand are described. As mentioned in chapter four, this hand consists of four motors of which the first three drive the thumb, forefinger and the middle finger of the hand while the fourth motor drives the two small fingers. Each of the fingers has one degree of freedom and is actuated by a power screw mechanism as shown in figure 5.1.
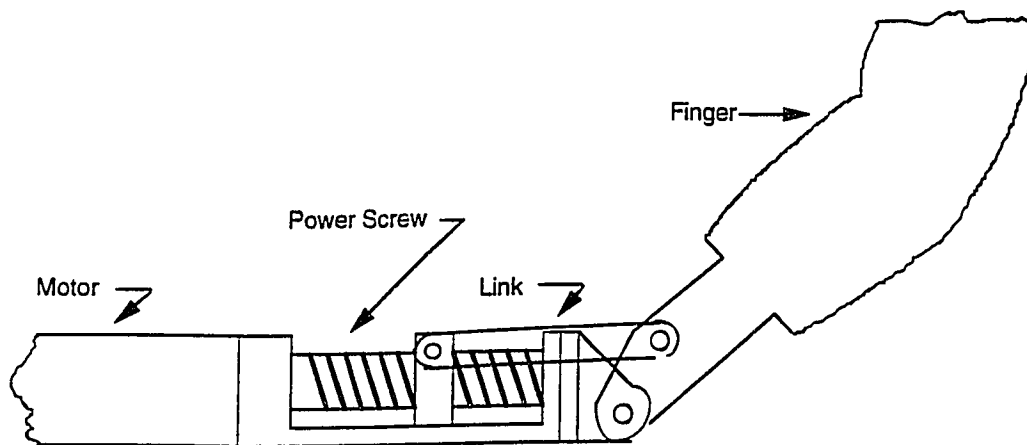
FIGURE 5.1: The Finger Actuator

We will start by deriving a dynamics model of the finger and consider moving the finger joint to a desired angle. Next, the stability of the equilibrium will be proved using Lyapunov stability criterion. Since the structure of and the method of actuation is

identical for all the fingers, this analysis is valid for all of the fingers.

5.2 GEOMETRY:

In figure 5.2, the symbols that are used in the following derivation are defined. The distance r between the fixed point about which the finger pivot and the point where the link has been connected to the finger has been exaggerated for clarity.
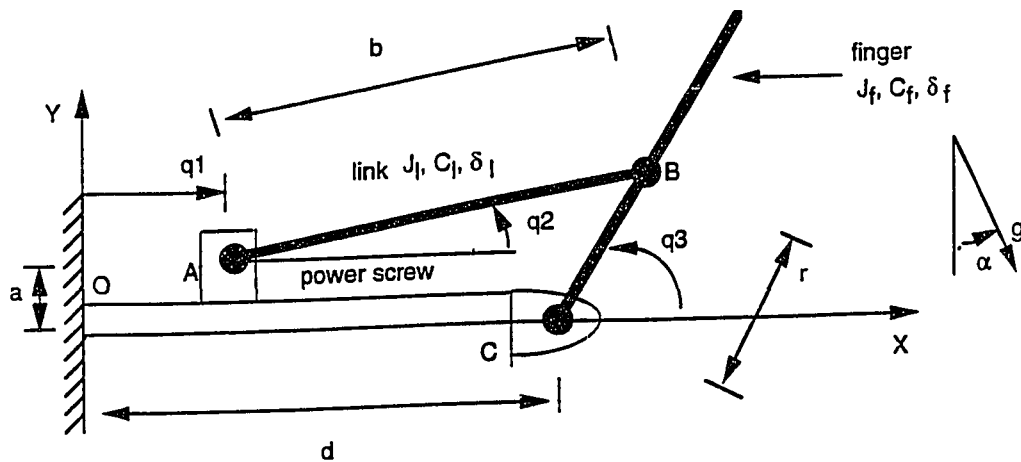
FIGURE 5.2: The definition of variables

By Geometry we get the following constraint equations relating q1, q2 and q3

$$q_1 + bCos(q_2) = d + rCos(q_3)$$
$$bSin(q_2) = rSin(q_3) - a$$

Due to the nature of the system, the angle q2 is very small (between -10 and 10 degrees). Due to this we can make the small angles approximation with little error. (Sin(q2)=q2 and Cos(q2)=1). Which gives the following simplified expression.

$$d + rCos(q_3) = q_1 + b$$
$$rSin(q_3) = a + b(q_2)$$

In the finger, there is a potentiometer attached to the power screw which allows us to measure q1. Therefore, we need to solve the above equations for q2 and q3 in terms of q1.

$$q_3 = Cos^{-1}(\frac{q_1 + b - d}{r})$$

$$q_2 = \frac{\sqrt{r^2 - (q_1 + b - d)^2} - a}{b}$$

(5.1)

5.3 DYNAMICS:

In the following analysis, the system has been divided into two sections. The power screw and the link combined are treated as a two link robot with forces F_x and F_y acting on it at the end

effector. (The end effector is the pivot where the link is connected to the finger) The resultant of F_x and F_y is the total force exerted by the finger on the link. In the second section the finger is considered as a one degree of freedom robot with F_x and F_y acting on it.

The distance to the center of mass of the link (AB) from A is defined to be C_l and the angle that the line from A to the c.m. makes to AB is defined to be δ_l. The moment of inertia of the link about its
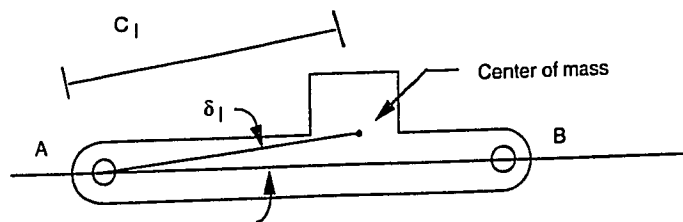
FIGURE 5.3: The link parameters

center of mass is defined to be J_l (figure 5.3). Similarly, the corresponding parameters for the finger are defined to be C_f, δ_f and J_f. We get the following expression for the kinetic energy of the two link robot. The masses of the link and the finger are defined to be m_l and m_f respectively.

$$K = \frac{1}{2}m_l[(\dot{q}_1 - \dot{q}_2 C_l Sin(q_2 + d_l))^2 + \dot{q}_2^2 C_l^2 Cos^2(q_2 + d_l)] + \frac{1}{2}J_l \dot{q}_2^2 + \frac{1}{2}m_s \dot{q}_1^2$$

$$= \frac{1}{2}m_l[(\dot{q}_1^2 - 2\dot{q}_1\dot{q}_2 C_l Sin(q_2 + d_l) + \dot{q}_2^2 C_l^2] + \frac{1}{2}J_l \dot{q}_2^2 + \frac{1}{2}m_s \dot{q}_1^2$$

Where m_s is the mass of the moving part in the power screw. The potential energy is given by,

$$V = m_l g C_l Sin(q_2 + d_l - a) + m_s g q_1 Sin(a)$$

By applying Lagranges equation,

$$\frac{d}{dt}\left(\frac{\partial L}{\partial \dot{q}_i}\right) - \frac{\partial L}{\partial q_i} = \tau_i$$

Where L=K-V, there are two components to the total force acting on the power screw. The first component of force due to the motion of the link, of the force acting on the power screw is denoted by F_1. And the second component due to the force at the end effector is denoted by F_2. Since the second joint is free, the total moment at the joint is zero. As with the first joint, there are two components to this moment. The first is due to the motion of the system denoted by T_{21} and the second due the force acting at the end effector denoted by T_{22}. Hence $\tau_1 = F_1$ and $\tau_2 = T_{21}$ and we get the following equations.

$$F_1 = (m_s + m_l)\ddot{q}_1 - m_l C_l \ddot{q}_2 Sin(q_2 + \delta_l) - m_l C_l \dot{q}_2^2 Cos(q_2 + \delta_l) - m_s g Sin(\alpha) \quad (5.2)$$

and for the second joint,

$$T_{21} = m_l C_l^2 \ddot{q}_2 - m_l C_l \ddot{q}_1 Sin(q_2 + \delta_l) + J_l \ddot{q}_2 + m_l g C_l Cos(q_2 + \delta_l - \alpha) \qquad (5.3)$$

In order to calculate F_2 and T_{22} we need to derive the Jacobian of the system. We get the following equations for the forward kinematics.

$$x = q_1 + bCos(q_2)$$
$$y = bSin(q_2)$$

By differentiating, we get the following,

$$\begin{bmatrix} \dot{x} \\ \dot{y} \end{bmatrix} = \begin{bmatrix} 1 & -bSin(q_2) \\ 0 & bCos(q_2) \end{bmatrix} \begin{bmatrix} \dot{q}_1 \\ \dot{q}_2 \end{bmatrix}$$

Therefore, the Jacobian is given by,

$$J = \begin{bmatrix} 1 & -bSin(q_2) \\ 0 & bCos(q_2) \end{bmatrix}$$

Now applying the equation, $\tau = J^T F$, where τ is the vector of joint torque's and F is the Force/Torque vector at the end effector, we get the following expression.

$$\begin{bmatrix} F_2 \\ T_{22} \end{bmatrix} = \begin{bmatrix} 1 & 0 \\ -bSin(q_2) & bCos(q_2) \end{bmatrix} \begin{bmatrix} F_x \\ F_y \end{bmatrix}$$

The mass and the inertia of the link and the mass of the moving part of the power screw are very small compared to the mass and the inertia of the finger. Therefore the components of the joint torque's and forces due to the motion of the link and power screw are negligible compared to the components due to the motion of the finger. Therefore $T_{21} = 0$ and hence $T_{22} = 0$ as the total is zero and also, $F_1 = 0$.

Hence $F_x = F_2$ and $F_y = F_x$ tan (q2). Therefore, the resultant of F_x and F_y denoted by $F_r = F_x$ Sec (q2). Hence, F_r acts along the link and the total force at the power screw F is given by,

$$F = F_1 + F_2 = 0 + F_r Cos(q2) = F_r Cos(q2) \qquad (5.4)$$

Next, we consider the motion of the finger and apply Newton's law for the moments about C. In the most general situation, there are three forces acting on the finger in addition to the forces at the joint. The first is due to gravity and the second is $-F_r$. In addition to these, there can be an external force acting on the finger tips. Let us denote the moment due to this as M_e. Hence we get the following equation.

$$-M_e + rSin(q_3 - q_2)F_r - C_f m_f gCos(q_3 - \delta_f - \alpha) = J_f \ddot{q}_3 \qquad (5.5)$$

From the motor model, we get the following equation relating the input voltage V, the motor armature angle θ and the load torque T.

We have ignored the inductance which is very small for the particular motor that was used (Micromotors, 1988).

$$\frac{J_m R}{K_i} \ddot{\theta} + \left(\frac{B_m R}{K_i} + K_b\right)\dot{\theta} + \frac{R}{K_i}T = V \qquad (5.6)$$

where J_m is the inertia of the motor and gearhead and B_m is the damping constant of the motor. K_i is the torque constant and K_b is the back e.m.f. constant. R is the armature resistance and V is the input voltage to the motor. From the power screw mechanism, θ is proportional to q1 and T is proportional to the force at the power screw, F. Therefore we get the following equation.

$$T = K_f F \text{ and,} \qquad (5.7)$$

$$\theta = K_q\, q1 \qquad (5.8)$$

where K_f is the constant of proportionality between motor torque and the force at the power screw which depends on the gearhead and the power screw parameters. K_q is the constant of proportionality between θ and q1 which would be equal to $1/K_f$ if there were no frictional losses. both these constants can be calculated.

5.4 CONTROL:

Grouping all of the relevant equations and rewriting equation (5.6) in a shorter form,

$$A\ddot{\theta} + B\dot{\theta} + T' = u$$

where, $A = \dfrac{J_m R}{K_i}$; $B = \dfrac{B_m R}{K_i}$; $T' = \dfrac{R}{K_i}(T + T_f)$; and $u = V$

Where T_f is the component of the torque at the motor due to friction which can be determined experimentally (section 5.5.2). All of the constants are known positive numbers. Using the measured value of q1, we can compute T on line using the following equations,

$$T = K_f F \quad \text{and,} \tag{5.7}$$

$$F = F_r Cos(q2) \tag{5.4}$$

$$-M_e + rSin(q_3 - q_2)F_r - C_f m_f g Cos(q_3 - \delta_f - \alpha) = J_f \ddot{q}_3 \tag{5.5}$$

The moment due to external forces M_e can be measured using the force sensors mounted on the finger. All of the constants are known and q2 and q3 can be calculated using the value of q1 from equations (5.1).

For this system we propose a PD control (treating T' as a disturbance) given by,

$$u = k_p(\theta^d - \theta) - k_d\dot{\theta} + T' \tag{5.8}$$

where θ^d is the desired finger joint angle. Consider the Lyapunov function candidate,

$$V = \frac{1}{2}A\dot{\theta}^2 + \frac{1}{2}k_p(\theta^d - \theta)^2$$

Differentiating,

$$\dot{V} = A\ddot{\theta}\dot{\theta} - k_p(\theta^d - \theta)\dot{\theta}$$

Substituting from (5.6),

$$\dot{V} = \dot{\theta}(u - B\dot{\theta} - T') - k_p(\theta^d - \theta)\dot{\theta}$$

Substituting for u-T' from (5.8),

$$\dot{V} = -B\dot{\theta}^2 + \dot{\theta}(k_p(\theta^d - \theta) - k_d\dot{\theta}) - k_p(\theta^d - \theta)\dot{\theta}$$

Therefore, we get,

$$\dot{V} = -B\dot{\theta}^2 - k_d\dot{\theta}^2 \leq 0$$

Therefore, the equilibrium, $\theta = \theta^d$ is stable. Additionally, as $\dot{V} = 0$ implies that the first and second derivatives of θ are zero, by substituting in equations (5.6) and (5.8), we get that $\dot{V} = 0$ implies $\theta = \theta d$ which proves invoking Lasalle's theorem that the system is asymptotically stable.

5.5 FRICTIONAL EFFECTS:

5.5.1 Efficiency:

The frictional losses in this system consist of the losses at the motor, the gearhead, the power screw and at the joints. The maximum efficiency of the motor according to the manufacturers data is 50 % and the published efficiency of the gearhead is around 80 %. Assuming a coefficient of friction of 0.15, our estimate of the efficiency of the power screw is around 33 % (This calculation has been included in Appendix C). Therefore the combined efficiency of the drive mechanism of the fingers, ignoring the losses at the joints is around 13 %.

5.5.2 Measuring the Term due to Friction in Equation 5.8:

The frictional term T_c in equation 5.8 was determined by disconnecting the finger at the link and then increasing the voltage into the motor until the position sensors indicated movement. Since the only load on the motor is due to the friction, this voltage gives us the load contribution due to static friction. The experiment was performed for a range of joint angles and the results indicated a range of 1.5 - 2.4 volts at the motor and was generally constant with local variations. However, the friction may become much larger at some locations. This was accounted for in the program as described in the next section.

5.6 THE GRAVITY EFFECTS:

Since the hand may be oriented at any angle with respect to gravity, the angle α in equation 5.5 is not known. Therefore, in the implementation of the control described in this chapter, we had to account for the variations in α. The problems due to the variations in α and Tc were solved by making the compensation term T' adaptive. If the sensors detected that the arm is stuck, the term T' is increased until the arm moved. Every 100 iterations, the term T' is brought back to the normal levels. Thus if the compensation became insufficient, due to variations in the effects of gravity and friction, the system is still capable of recovering.

5.7 SUMMARY:

We started by deriving the geometric constraints of the system and then derived the equations of motion using the Lagrangian method. For this system we propose a PD control with compensation. Next we proved the stability of the equilibrium $\theta = \theta^d$ using Lyapunov stability. Due to friction, we estimate the efficiency of the drive mechanism to be less than 13 %. The variations in the compensation term was accounted for in the algorithm by making it adaptive.

CHAPTER 6: THE ALGORITHM

6.1 INTRODUCTION:

In this chapter, the algorithm that is used to achieve the objective of this research project and implement a grasp of desired strength is described. The results of the experiments performed with the system will also be presented. Finally the results will be discussed.

6.2 THE STEPS IN GRASPING:

The grasping process was divided in to three parts.

(1)   Grasp initiation

(2)   Closing in

(3)   Holding the object

During the grasp initiation phase, the fingers move under PD control (as described in chapter 5) from the current configuration to a desired configuration that depends on the particular grasp selected. The desired configuration opens the hand wide to allow grasping objects of any size. In the second phase the fingers move in on the object until the force sensors indicate contact. Once the object

is in contact, the system enters in to the third phase where the system maintains a desired level of force at the force sensors.

6.2.1 Grasp Initiation:

As mentioned in the previous section, during grasp initiation, the fingers move from their current joint positions to a desired configuration. The desired configuration depends on the particular grip. For example, for the cylindrical grip, the thumb moves to a position that opposes the other four fingers and they open wide to allow for grasping cylindrical shaped objects. The joint angles corresponding to each grip have been measured and hard coded in the program. In the algorithm, the desired voltage inputs to each of the motors are calculated from equation 5.8. The gains kp and kd have been adjusted to make the system critically damped.

6.2.2 Closing In:

During this phase, the fingers are made to move in until any one of the force sensors installed in the fingers that are moving in detects a force. If the fingers do not detect any force and the finger have moved the full range (this would happen if there is no object) then the system returns to the starting state. If on the other hand an object has been detected, the system enters the next phase. The moving in is also done under PD control as in the initiation phase by

breaking up the motion into several segments. Every one hundred iterations, the system calculates a new desired position by multiplying the time taken for one hundred iterations by the desired velocity for each finger.

6.2.3 Holding the Object:

During this stage, the fingers move (independently) to maintain the desired level of force at the force sensors. Based on the users intent the system computes a low and a high for the forces. If the forces on all of the sensors in a finger are below the low level the finger is closed in to increase the forces. On the other hand if any of the sensors record a level of force higher than the high level, the finger is opened to decrease the force.

The opening and closing of the fingers is done by setting the voltage into the motor at a maximum for a fixed length of time during each iteration. Due to the relatively large range of force allowed, this method worked without causing the system to oscillate.

6.3 THE RESULTS:

At the time of the experiment, the hand had been programmed to achieve completely only one grasp. The other grasps were partly completed. However, since the concept and the procedure is the same for all grasps, it was sufficient to perform the experiments with one grasp. The particular grasp that was completed was not one of the standard grasps and we called it the cup grasp. The cup grasp is very similar to the cylindrical grasp except, only the fore finger and the middle finger close in on the object where as in the cylindrical grasp, all four fingers move in. In the cup grasp, the two small fingers are held at a half open angle which allows them to support a large cup if necessary. The program printed the sensor readings on the screen which allowed us to monitor the controller.

In the first experiment, the hand was made to hold a Styrofoam cup at the three levels of force. During the second experiment, the hand was made to grasp a relatively heavy cylindrical wax rod with the three levels of force. The rod was too thin for it to be supported by the two small fingers and therefore the hand had to apply enough force at the fingertips of the fore finger and middle finger to hold it.

In the first experiment, the hand was able to hold the Styrofoam cup gently with a low level of force. With medium and high levels of force the hand deformed the cup as expected. At the

high level of force, it caused some damage. In the second experiment, the hand was able to hold the wax rod without slipping (even when we tried to snatch it from the hand) with the high and medium levels of force. With the low level of force the rod tended to slip as expected.

The following are some of the observations made during the experiments and before.

(1) The sensors tend to drift. That is, when a force is applied and kept constant the reading in the sensor keeps increasing. This effect was minimized in this system by having discrete levels of force. This made it necessary for the sensor to drift a considerable amount before it could affect the reading in the grasping program.

(2) When a large force was applied and removed, some of the sensors took some time to recover.

(3) Occasionally the sensors erroneously showed a low level of force when there was no object in contact .

(4) The hand could not deliver more than one pound of force at the ingertip. This made it difficult for the hand to achieve the hard grasp at times.

6.4 DISCUSSION:

The results of the first and second experiments clearly demonstrate the usefulness of tactile sensing in a prosthetic hand. We could adjust the desired force levels to suit the day to day tasks of the prosthesis. The number of levels of force can also be extended to suit the needs of the user (provided we can distinguish these levels of force from the myoelectric signals).

One important observation is that even though our tactile sensor was capable of providing both the magnitude and the location of force, we did not use location information in this algorithm. The control strategy that we used to maintain the force did not require us to calculate the moment due to the external forces. If we need only to maintain the external forces within a range that is relatively wide, we do not need to know the exact location of force. This could help us reduce the cost in terms of weight and power considerably. In this case we can have one force sensor for each motor. However, this one force sensor needs to cover the entire finger. One possible approach is to have several sensors in the finger and have them connected in parallel.

On the other hand, if we need to control the force more accurately at some stage and we need to use a control strategy that requires the computation of the desired moment at the finger joint, then we would need to have several force sensors for each finger as in this hand.

The drift in the response is a property of Force Sensitive Resistors. This is one of the biggest drawbacks to using Force Sensitive Resistors and quantifying these properties could be a useful and interesting research problem. The delay in recovering from a large force is probably due to faulty installation.

The occasional readings of force when there was no object in contact was caused by the combined effects of the glove pre-loading the tactile sensors and the drift in the sensors. We compensated for the pre-loading of the sensors in the program. However, due to the drift in the sensors and variations in the level of pre-loading, occasionally the force sensors displayed force when there was no object in contact. One solution is to increase the level of compensation in the program such that the system will not record force unless there is an object in contact. The problem with this is that it reduces the sensitivity of the system. In the program, when we make the decision of whether an object is in contact or not, we add the forces of all three sensors and decide that an object is in contact only if the total is greater than or equal to two. Thus program is capable of handling one stray reading. However, it does have problems with stray readings when it's trying to maintain the forces within the desired range in the third part of the grasping algorithm.

The inability of the hand to deliver more than one pound of force demonstrates some of the mechanical shortcomings of this hand. This hand was built for the purpose of testing tactile sensors

and is not very reliable. Also it has a very low efficiency (section 5.5.1) which will result in low battery life. Reliability and battery life are the two of the biggest concerns of prosthetic hand users These issues must be addressed in future developments of prototype myoelectric hands. The advantage of having a power screw is, it's self locking. This makes it possible to keep the motors turned off most of the time and thereby save energy. However, due to the low efficiency of the power screw it may be less costly to have a more efficient gearhead and a brake.

6.5 SUMMARY:

The algorithm used to achieve the desired grasps and the experimental results were presented in this chapter. The grasping algorithm consists of three steps. In the first step, the fingers are made to move under PD control to a desired configuration. During the second step, the fingers move in until the sensors detect force. In the third stage the fingers are moved such that the forces at the finger/ object interface are maintained within the desired range.

The experiments demonstrated that the system is able to grasp a delicate object (Styrofoam cup) gently with a low level of force and a hard, heavy object with the hard grasp. Some of the problems in the sensors were due to a few undesirable properties of conductive rubber.

CHAPTER 7: CONCLUSIONS AND FUTURE EXTENSIONS

7.1 INTRODUCTION:

In this chapter, the entire research project is summarized. In section 7.3 the conclusions that can be drawn from this project are presented. The last part of this chapter suggests some possible extensions to this research.

7.2 SUMMARY:

With the development of myoelectric control, powered prosthetic hands became popular. Even though a considerable amount of progress has been made in myoelectric control, the hands that are currently available provide little or no sensory feedback and have limited functionality. This creates a considerable limitation to the kinds of objects that can be grasped. The purpose of the myoelectric hand project at Rice University is to reduce some of these limitations.

In order to achieve this objective we must improve several components of the hand. The functionality of the hand must be increased. We need to be able to obtain more information from the myoelectric signals. A system of sensors and a method to interpret

the sensory information needs to created. Finally, we need a method to display the relevant sensory information to the user. Out of these, we chose to concentrate on creating a hand with a suitable set of sensors and creating a method to interpret this information while other researchers concentrate on the other aspects.

The hand we built consist of four motors, four position sensors and eleven force sensors and the circuitry to interface them to an IBM 386 PC. After considering several designs of sensors we chose to use Force Sensitive Resistors made by Interlink Electronics. The sensors were calibrated at several discrete levels of force. This allowed us to know the range of forces acting on the sensors.

After considering the dynamics of the system, we decided to use PD control with compensation to make the finger move to the desired position. The compensation was allowed to adaptively change in order to make the system capable of handling the changes in the motor torque due to variations in friction and the variations in gravitational terms (due to the changes in the orientation of the hand).

The algorithm used to grasp objects with this system consists of three sections. In the first section, the fingers are made to move under PD control to a desired configuration. During the second part, the fingers move in until the sensors detect force. In the third section the fingers are moved such that the forces at the finger/object interface are maintained within the desired range.

During the experiments, the system was able to grasp a delicate object (Styrofoam cup) gently with a low level of force and a hard, heavy object with the hard grasp demonstrating the ability to control the grasp forces. Some sensors showed a delay in recovering from a large force. This was probably due to problems in the installation. The sensors also tended to drift. This is one of less desirable properties on Force Sensitive Resistors. Once the gains Kp and Kd were adjusted to the correct level, the hand was able to achieve the desired configuration under PD control using the potentiometers in the first stage of the algorithm. We were also able to make the fingers move in on the object at the desired speed in the second stage of the grasping process.

The reason for needing a large number of sensors is the need to be able to know both the magnitude of the force and its location. However, in this project we did not use the location information and still managed to maintain the forces within the desired range. This suggests the possibility of reducing the number of sensors.

7.3 CONCLUSIONS:

(1)   If it is sufficient to maintain the contact forces within a range, then the number of force sensors can be reduced considerably.

(2)   The system of sensors have the following short comings.

1. The response tends to drift.

2. Some sensors showed some delay in recovering from large forces.

The drift is a property of the sensors that were used. The delay in response was caused by errors in installation.

(3) There is a trade off between reliability and sensitivity for these sensors due to the pre-loading effects of the glove.

(4) We were able to achieve the desired response from the system under PD control.

(5) This hand which was built for testing tactile sensors is not very efficient and it is limited in its ability to execute very hard grasps. However, it permitted demonstrations that showed the ability of the sensors and algorithm to control grasp force.

7.4 FUTURE EXTENSIONS:

Even though we managed to control the grasp forces with this system, there is much work left to be done before this type of system can be produced commercially. We have ignored some of the most important constraints in this project. Among these are, size, weight and power constraints in a prosthesis. The computers that are small enough in terms of size and power consumption to fit

inside a prosthesis does not have the computational power and the memory that an IBM PC has. In addition some of the circuitry used in this project need to be replaced by simpler, smaller circuits. In addition, the sensors need to be more reliable. Combining all of the components mentioned in chapter two together and building a complete system within the constraints mentioned above could be an interesting and useful extension to this work.

The problems with the sensors that were discussed earlier are a major obstacle towards their application to prosthetic and robotic devices. It is possible that if we can come up with a good mathematical model of the sensor, we may be able to predict the response of the sensors based on their physical parameters. Such a model could be very useful in the designing and application of these sensors. This is another possible extension to this research.

One very important aspect that was not covered during this research is slip detection. As mentioned in chapter two, there are two methods of detecting slip. The first method is to create a sensor that is capable of detecting the vibrations caused by slip while the second method is to look at the movement of the tactile image on an array of sensors. It would be useful to explore alternative methods of detecting slip. It may also be possible to use some of the methods described in sensory fusion to get a better estimate of slip by combining the information from several sensors. This is another possible extension to this research.

Display devices (mentioned in chapter two) are important both for prosthetic devices and teleoperation and there is still much work to be done in this area. It may also be possible to combine several methods to provide better feedback to the user. Some methods which
are not suitable for frequent use can be used to display less frequent information such as the detection of slip. This is another important extension to this research.

7.5 CHAPTER SUMMARY:

In this chapter, the material presented in this thesis was summarized and the following conclusions were drawn. If the forces need only to be maintained within a relatively large range, the number of sensors can be reduced. The sensors tend to have the problems of hysteresis, drift and delay in recovery and there is a trade off between reliability and sensitivity in these sensors due to the pre-loading effect of the glove. We were able to achieve the desired response from the system under PD control for moving the fingers and the hand demonstrated the ability to control the grasp forces using the current set of sensors. Finally, some possible future extensions to this research were presented.

REFERENCES

[1] Baker, A, Caffrey, M., Cue, M., Smith, A., Baker, A. and Speciale, S. "Myoelectric prosthesis for Below-Elbow Amputation" MECH 407 report, Department of Mechanical Engineering and Material Science, Rice University, 1993.

[2] Bochard, M., Gacht, H., Radike, R., Sauerbruch, F. and Schlesinger, G. "Ersatzglieder und Arbeitshilfen" Berlin, Springer, 1919.

[3] Chappell, P.H. and Kyberd P.J. "Object-slip Detection During Manipulation Using a Derived Force Vector", Mechatronics, 12, p.1-13, 1991.

[4] Dalsey, R., Gomez, W., Seitz, W.H. Jr., Dick, H.M., Hutnick, G. and Arkdeniz, R. "Myoelectric Prosthetic replacement in the upper-extrimity Amputee" Orthapaedic Review, vol. xviii, No. 6, June, 1989.

[5] Dario, P., Bergamasco, M. and Fiorillo, A. "Force and Tactile Sensing for Robotics" in Sensors and sensory systems for advanced robots Ed. P. Darrio and C.E. Piaggio, Springer-Verlag, Berlin, 1988, p. 153-181, 1988.

[6] deFlorez, L. "True Blind Flight" in the Journal of the Aeronautical Sciences, Vol. 3, p. 168-170, 1936.

[7] Farry, K. A. and Walker, I.D. "Myoelectric Teleoperation of a Complex Robotic Hand" Proc. IEEE International Conference on Robotics and Automation, p. 502-509, 1993.

[8]   Giampapa, V., "A prosthetic hand with tactile sensitivity", Sensors, p. 43-44, January 1989.

[9]   Grisham, J. P., "A Modular Fingertip Design for Normal Force Feedback Control of a 3-Fingered Dexterous Robotic Hand" M.S. Thesis in Mechanical Engineering, Rice University, 1992.

[10]   Harmon, L.D. "Automated Tactile Sensing" International Journal of Robotics Research, 1 (2), p. 3-32, 1982.

[11]   Hortensius, P. and Onyshko, S. "Microcomputer-based Prosthetic Limb Controller: Design and Implementation" Annals of Biomedical Engineering, Vol. 15, p. 51-65, 1987.

[12]   Interlink Electronics A Tech Note: Suggested Electrical interfaces for Force Sensing Resistors, Interlink Electronics, Camarillo, California, 1994.

[13]   Interlink Electronics, FSR ^{TM} Technical Specifications, Rev 81151891, August, Interlink Electronics, Camarillo, California, 1989.

[14]   Interlink Electronics, Technical Overview, "Electrical Interfacing" February, Interlink Electronics, Camarillo, California, 1990.

[15]   Kaczmarek, K. A., Webster, J.G., Bach-y-Rita and Tompkins, W.J. "Electrotactile and Vibrotactile Displays for Sensory Substitution Systems" <u>IEEE transactions on Biomedical Engineering</u>, Vol. 38, no 1, p. 1-15, January, 1991.

[16]   Kato, I, Yamakawa, S, Ichikawa K. and Sano, M. "Multifunctional Myoelectric hand with pressure sensory feedback -- Waseda Hand 4P", <u>Proc. of the International Symposium on External Control of Human Extremities</u>, Dubrovnik, Yugoslavia, p. 155-170, August 25-30, 1969.

[17]   Knox, E.H., Childress, D.S. and Heckathorne, C.W. "Slip Detection and Automatic Grasping for a Prosthetic Prehensor", <u>Proc. Seventh World Congress of ISPO</u>, p. 189, June-July, 1992.

[18]   Kyberd, P. and Chappel, P.H. "Characterization of an Optical and Acoustic Touch and Slip Sensor for autonomous manipulation", p. 969-975, <u>Measurement, Science and Technology</u>, V. 3, 1992.

[19]   Ledar, S. B., Spitzer, J.B., Milner, P. Flevaris-Phillips, C. and Richardson, F. "Vibrotactile Stimulation for the Adventitiously deaf: An Alternative to Cochlear Implantation" <u>Arch. Physical Med. Rehabilitation</u>, Vol. 67, p. 754-758, 1986.

[20] Massimino, M.J. "Sensory Substitution for force Feedback in Space Teleoperation" Ph.D. Thesis, Massachusetts Institute of Technology, 1992.

[21] Micro Mo Electronics Inc. "Miniature Drive Systems" Micro Mo Electronics Inc., St. Petersburg, Florida,1990.

[22] Moss-Salentijn, L. "The Human Tactile System" in Advanced Tactile Sensing for Robotics Ed. by Nicholls, H.R., Publ. World Scientific, Singapore, p. 123-144, 1992.

[23] Näder, Dr.-Ing E.H. "The Artificial Substitution of Missing Hands With Myoelectric Control" Clinical Orthapaedics and Related Research, Number 258, p. 9-17, September, 1990.

[24] Nicholls, H.R. "Tactile Sensor Designs" in Advanced Tactile Sensing for Robotics. Ed. by Nicholls, H.R., Publ. World Scientific, Singapore, p.13-40, 1992.

[25] Reiter, R. "Eine Neu Electrokunstand" Grenzgebeite der Medicine, 1, 4, p. 133-135, 1948.

[26] Seow, K.C. "Capacitive Sensors" in Tactile Sensors for Robotics and Medicine. Ed. John G. Webster, New York, John Wiley & Sons, p.192-222, 1988.

[27] Scott R.N., Brittain, R.H., Caldwell, R.R., Cameron, A.B. and Dunfield, V.A. "Sensory-feedback system compatible with myoelectric control", Medical & Biological Engineering & Computing , p. 65-69, 1980.

[28] Scott, R.N. and Parker, P.A. "Myoelectric Prosthesis State of the Art" in Journal of Medical Engineering Technology, Volume 12, number 4, p. 143-151, 1988.

[29] Silvermintz, Larry "Optioelectronic Sensor" in Tactile Sensors for Robotics and Medicine, Ed. John G. Webster, New York, John Wiley & Sons, p.223-244, 1988.

[30] Welch, R. B. and Warren, D.H. "Intersensory Interactions" in Hand book of Perception and Human Performance, Chap 25. Eds. K.R. Boff, L. Kaufman and J.P. Thomas, New York: John Wiley and Sons, 1986.

[31] Winkler, W. and Bierwirth, W. "The use of a gliding detector for control of prosthesis-hand" Proc. Seventh World Congress of ISPO, June-July, p. 188, 1992.

APPENDIX A: COMPUTER PROGRAMS

A.1 Grasp.h:

```
/*****************************************************************
*                                                               *
*          Programmed by: Ruvinda Gunawardana                   *
*                                                               *
*****************************************************************/


#include <stdio.h>
#include <stdlib.h>
#include <bios.h>
#include <dos.h>
#include <time.h>
#include <graph.h>
#include <math.h>
#include <float.h>
#include <signal.h>
#include <conio.h>
#include <memory.h>


/*

        Parallel Port Definations for our setup of the homebrew card It
        uses the Intel 8255 PIO chip PA, PB, PC are the programmable
        registers CO is the control register. These are mapped into the
        I/O space of the PC

*/
#define IO_BASE_ADDR                    0x360
#define PA                              IO_BASE_ADDR
#define PB                              IO_BASE_ADDR+1
#define PC                              IO_BASE_ADDR+2
#define CO                              IO_BASE_ADDR+3
#define STOP_ALL                        18
#define SETUP_PIO                       0x90


/* The following are definitions of the subroutines in this system
*/

void setupPioBoard(void);
void stop_motors(void);
void dummy(void);

void read_sensors( int s[15] );
void display( int s[15] );

void initiate_grasp(char *g, int *panic);
void close_obj(char *f, char *g, int *panic);
void hold_in(char *f, char *g, int *panic);
```

A.2   Grasp1.c:

```
*********************************************************************
*                                                                 *
*         Programmed by: Ruvinda Gunawardana                       *
*                                                                 *
*********************************************************************/

/* This file contains the first part of the program that implements the
   grasping algorithm described in chapter 6.
*/


#include "grasp.h"


main(){

   int s[15], i, n=1, panic = 0;
   double t;
   char in_ch, f, g;

   clock_t start_t, end_t;

   setupPioBoard();

   stop_motors();

   start_t = clock();


/* In this loop, after printing the display on the screen
   the relevent subroutines are called based on the users
   input.
*/

   do{

      system("cls");
      _settextposition(0,1);

      printf(" The Myoelectric Hand Project");
      printf("\n Department of Mechanical Engineering");
      printf("\n Rice University.   April, 1994 ");
      printf("\n Programmed by Ruvinda Gunawardana");
      printf("\n\n Press one of the following keys to select the correspondir
      printf("\n Or any other key to exit");
      printf("\n\n o - open palm   c - cup   k - key   t - Three pt.");

      do{

         n++;
         read_sensors( s );
```

```
        if( n%100 == 0) display(s);
        end_t = clock();


    }while(!kbhit());


    g = getch();

    if(g =='c'|| g=='C' || g=='t' || g=='T'|| g=='k' || g=='K' ){
        _settextposition(6,1);

        if(g == 'c'|| g == 'C')printf("Cup");
        if(g == 't'|| g == 'T')printf("Three pt. ");
        if(g == 'k'|| g == 'K')printf("Key ");


        printf(" grasp selected.              Enter the force level              \n");
        printf("
        printf(" 1 - Soft        2 - Medium        3 - Hard      Other key - Redo ");

        do{
        }while(!kbhit());

        f=getch();


        if((f=='1')||(f=='2')||(f=='3')){

/* Initiating grasp */

            _settextposition(6,30);
            if(f=='1')printf("Soft ");
            if(f=='2')printf("Medium ");
            if(f=='3')printf("Hard ");
            printf("force level selected                          \n " );

            _settextposition(9,1);
            printf("Status:  Initiating Grasp,                                    ");
            panic=0;
            initiate_grasp(&g, &panic);

/* Closing in on the object   */

            if(panic==1){ stop_motors(); break; }
            _settextposition(9,1);
            printf("Status:  Closing in                        " );
            panic=0;
            close_in(&f, &g, &panic);

/* Holding object   */

            if(panic==0){
                _settextposition(9,1);
                printf("Status:  Holding object                   " );
                panic=0;
                hold_obj(&f, &g, &panic);

            }
```

```
        }
      }
      else if(g == 'o' || g == 'O'){
        _settextposition(9,1);


        printf("Status: Open palm                              " );
        initiate_grasp(&g, &panic);
      }
      else
       panic = 1;

      if(panic == 1){
        stop_motors();
        break;
      }


    }while(1);

    system("cls");


}



/* This subroutine reads in the force and position sensors.
   The matrix b contains the calibration results which will
   be used to convert the voltage to lbs.
*/

void read_sensors( int s[15] )

{

  int i,j;

  int b[11][5] = {{ 25, 49, 58, 72, 157 },
                  { 60, 106, 158, 172, 185 },
                  { 50, 60, 70, 80, 135 },
                  { 20, 82, 114, 175, 222 },
                  { 70, 80, 90, 110, 195 },
                  { 10, 72, 160, 200, 236 },
                  { 40, 132, 167, 207, 232 },
                  { 75, 97, 143, 175, 209 },
                  { 60, 70, 80, 90, 110 },
                  {  0, 76, 160, 200, 225 },
                  { 65, 75, 85, 95, 104 }, };


  for(i=0;i<8;i++){

      outp(PB, 120+i);

      for(j=0;j<70;j++);

      outp(PB, 96+i);
```

```c
        for(j=0;j<70;j++);

        outp(PB, 104+i);

        for(j=0;j<70;j++);

        outp(PB, 24+i);

        for(j=0;j<70;j++);

        s[i] = inp(PA);

        for(j=0;j<70;j++);

        outp(PB, 56+i);

        for(j=0;j<70;j++);

        s[i+8] = inp(PA);

    }

    s[0] = 255 - s[0];

    for(i=4;i<15;i++){

        if ( s[i]<=b[i-4][0] ) s[i]=0;
        if ( (s[i]>b[i-4][0]) && s[i]<=b[i-4][1] ) s[i]=1;
        if ( (s[i]>b[i-4][1]) && s[i]<=b[i-4][2] ) s[i]=2;
        if ( (s[i]>b[i-4][2]) && s[i]<=b[i-4][3] ) s[i]=3;
        if ( (s[i]>b[i-4][3]) && s[i]<=b[i-4][4] ) s[i]=4;
        if ( s[i]>b[i-4][4] ) s[i]=5;

    }
}

/*  This subroutine displays the sensor readings on the screen
*/


void display( int s[15] )

{
    _settextposition(12,2);

    printf("Current sensor readings : \n ");
    printf("                                                Positions:

    printf("\n                %2d                              Thumb : %3d
, s[4],s[0]);
    printf("\n                **   ");
    printf("\n        **%2d", s[5]);
    printf("\n    ************ ");
    printf("\n ******************%2d *****%2d ******%2d *            Fore : %3c
,s[7],s[6],s[1]);
    printf("\n ****************");
    printf("\n ********************%2d *****%2d *****%2d *           Middle : 9
s[11],s[10],s[9],s[2] );
    printf("\n ****************");
    printf("\n ***********************%2d ******%2d *            Small : %3c
```

```
      ,s[12],s[3]);
      printf("\n ****************");
      printf("\n ******************************%2d *",s[14]);
}


/*  This subroutine sets up the I/O board
*/

void setupPioBoard(void)
{
  outp(CO, SETUP_PIO);
  outp(PB, 0x78);
   outp(PC, 0x00);
}


/* This subroutine stops all of the motors
*/


void stop_motors(void)

{


    _settextposition(1,60);


    outp(PC, 0x00);
    dummy();
    outp(PC, 0x20);
    dummy();
    outp(PC, 0x40);
    dummy();
    outp(PC, 0x60);

}



/*  This is a delay subroutine that is used to provide the necessary
    gaps in between consecutive commands to the motors.
*/



void dummy()
{
  int a;

  for (a = 1; a < 300; a++);

}
```

A.3 Grasp2.c:

```
/*


   This file contains the second part of the program that implements
the grasping algorithm described in chapter 6. The first subroutine
initiate_grasp implents the first step in the algorithm. The second
subroutine, close_in implements the second step and the third subroutine
hold_obj implements the third step.

*/


#include "grasp.h"

void initiate_grasp(char *g, int *panic)

{

  int xd[4], x[15], xp[4], fr[4], fr0[4], er[4], n=1, i, j, u, pan[4], erx[4];

  double  kp[4], kd[4], v[4], vd[4], t_fifty, t_ten;

  clock_t prev_t_f, prev_t_t,  t;


  if(*g=='c'|| *g=='C'){   xd[0] = 140; xd[1] = 140; xd[2] = 170; xd[3] = 50; }

  if(*g=='t'|| *g=='T'){   xd[0] = 140; xd[1] = 65; xd[2] = 100; xd[3] = 145; }

  if(*g=='o'|| *g=='O'){   xd[0] = 240; xd[1] = 185; xd[2] = 210; xd[3] = 145; }

  if(*g=='k'|| *g=='K'){   xd[0] = 240; xd[1] = 12; xd[2] = 210; xd[3] = 145; }


kp[0] = 0.65; kp[1] = 0.65;  kp[2] = 0.65; kp[3] = 0.6;
kd[0] = 0.4; kd[1] = 0.8; kd[2] = 0.9; kd[3] = 0.8;

fr0[0] = 10; fr0[1] = 8; fr0[2] = 8; fr0[3] = 8;
for(i=0;i<4;i++){er[i]=0; v[i]=0; pan[i]=0; fr[i]=fr0[i];}

t = clock();
prev_t_f = t;
prev_t_t = t;

read_sensors(x);


do{

  read_sensors(x);
```

```
for(i=0;i<4;i++){

  for(j=1;j<5;j++) dummy();

  erx[i] = xd[i] - x[i];

  u =(int) ( kp[i]* ( (double) erx[i] ) - kd[i]*v[i] ) ;


  if(u>0.8){
    u = u + fr[i];
    if(u>15)u=15;
    outp(PC,32*i+u);
  }
  else{

    if(u<-0.8){
      u = u - fr[i];
      if(u<-15)u=15;
      else u=-u;
      outp(PC, 32*i+16+u);
    }
    else outp(PC, 32*i);
  }

}


if(n%10==0){

  t = clock();

  _settextposition(1,40);

  t_ten = (double) (t-prev_t_t);

  for(i=0;i<4;i++){

    v[i] = ( (double) (x[i]-xp[i]) ) / (t_ten);
    xp[i] = x[i];

    if((erx[i]*erx[i]) < 25 )er[i]=0;
    else
    {
      if( (v[i] > 0.05 && erx[i] > 0 ) || ( v[i] < -0.05 && erx[i] < 0 ))er[i]=
      if(v[i]* v[i] <= 0.0025) fr[i]+=2;
      if( (v[i] > 0.05 && erx[i] < 0 ) || ( v[i] < -0.05 && erx[i] > 0 ))er[i]=

    }
```

```
      }

      prev_t_t = t;

   }



   if(n%150==0){

      j=0;
      for(i=0;i<4;i++){


         if(er[i]==1){
            pan[i]++;
            if(pan[i] > 2){
               _settextposition(9,50);
               printf(" motor %d not responding",i );
               stop_motors();
               *panic=1;
               break;
            }
         }
         else{

            j++,
            pan[i]--;
            fr[i]=fr0[i];
         }

         display(x);
         er[i] = 1;


         t = clock();

         t_fifty = (double) (t - prev_t_f);


      }


      _settextposition(9,50);
      if(j==4)printf("                         ");
      prev_t_f = t;

   }


   if(kbhit()){
      *panic=1;
      break;
   }
```

```
        if( erx[0]*erx[0] < 25 &&  erx[1]*erx[1]<25 && erx[2]*erx[2]<25 && erx[3]*erx[
            stop_motors();
            break;
        }


        if(*panic==1){
            break;
        }

        n++;

    }while(5);

    stop_motors();

}




void close_in(char *f, char *g, int *panic)

{

    int xd[4], x[15], xp[4], xmin[4], fr[4], er[4], n=1, i, j, u, pan[4], erx[4], ft

    double  kp[4], kd[4], v[4], vd[4], t_fifty, t_ten;

    clock_t prev_t_f, prev_t_t,  t;


  if( *g == 'c'|| *g== 'C' ) { vd[0] = 0.0; vd[1] = -0.02; vd[2] = -0.018; vd[3]=0.
  if( *g == 't'|| *g== 't' ) { vd[0] = 0.0; vd[1] = -0.015; vd[2] = -0.016; vd[3]=0.

   if( *g == 'k'|| *g== 'K' ) { vd[0] = -0.04; vd[1] = 0.0; vd[2] = 0.0; vd[3]=0.0;}

   if(*g=='c'|| *g=='C'){xmin[0] = 190; xmin[1] = 25; xmin[2] = 50; xmin[3] = 60; }
   if(*g=='t'|| *g=='T'){xmin[0] = 145; xmin[1] = 20; xmin[2] = 50; xmin[3] = 155; }
   if(*g=='k'|| *g=='K'){xmin[0] = 185; xmin[1] = 20; xmin[2] = 215; xmin[3] = 165;


   kp[0] = 0.6; kp[1] = 0.4;  kp[2] = 0.6; kp[3] = 0.6;
   kd[0] = 0.4; kd[1] = 0.85; kd[2] = 0.95; kd[3] = 0.8;


   fr[0] = 10; fr[1] = 7; fr[2] = 8; fr[3] = 8;

   for(i=0;i<4;i++){ er[i]=0; v[i]=0; pan[i]=0; }

   t = clock();
   prev_t_f = t;
   prev_t_t = t;

   read_sensors(x);
```

```
for(i=0;i<4;i++)xd[i] = x[i] + vd[i]*350;

do{

  read_sensors(x);

  for(i=0;i<4;i++){

    for(j=1;j<5;j++) dummy();

    erx[i] = xd[i]-x[i];
    u =(int) ( kp[i]* ( (double) (erx[i]) ) - kd[i]*v[i] ) ;

    if(u>0.5){
      u = u + fr[i];
      if(u>15)u=15;
      outp(PC,32*i+u);
    }
    else{

      if(u<-0.5){
        u = u - fr[i];
        if(u<-15)u=15;
        else u=-u;
        outp(PC, 32*i+16+u);
      }
      else outp(PC, 32*i);
    }

  }


if(n%10==0){

  t = clock();

  _settextposition(1,40);

  t_ten = (double) (t-prev_t_t);

  for(i=0;i<4;i++){

    v[i] = ( (double) (x[i]-xp[i]) ) / (t_ten);
    xp[i] = x[i];

    if( (erx[i]*erx[i]) < 25 )er[i]=0;
    else
    {
      if( (v[i] > 0.05 && erx[i] > 0 ) || ( v[i] < -0.05 && erx[i] < 0 ))er[i]=
      if(v[i]* v[i] <= 0.0025) fr[i]++;
      if( (v[i] > 0.05 && erx[i] < 0 ) || ( v[i] < -0.05 && erx[i] > 0 ))er[i]=
    }
```

```
      }

   prev_t_t = t;

}


if(n%100==0){

   for(i=0;i<4;i++){

      if(er[i]==1){
         pan[i]++;
         if(pan[i]>2){
            _settextposition(9,50);
            printf(" motor %d not responding",i );
            stop_motors();
            *panic = 1;
           break;
         }
      }
      else{
         pan[i]=0;
      }

      display(x);
      er[i] = 1;
      fr[0] = 10; fr[1] = 7; fr[2] = 8; fr[3] = 8;


      t = clock();

      t_fifty = (double) (t - prev_t_f);

      xd[i] = x[i] + (int) ( vd[i] * t_fifty);

      if(x[i]<xmin[i])xd[i] = x[i];

   }

   _settextposition(9,50);
   prev_t_f = t;
}


if(kbhit()){
   *panic=1;
   break;
}


if(x[0]<xmin[0] && x[1]< xmin[1] && x[2]<xmin[2] && x[3]<xmin[3] ){
   stop_motors();
   *panic = -1;
   _settextposition(9,47);
   printf("The object is too small or missing");
   printf("\n
   printf("\n  Press Any key to continue
   printf("\n
```

```
      do{
      }while(!kbhit());
      break;
   }

   ftot = 0;
   if(vd[0]!=0.0)ftot += x[4]+x[5];
   if(vd[1]!=0.0)ftot += x[6]+x[7]+x[8];
   if(vd[2]!=0.0)ftot += x[9]+x[10]+x[11];
   if(vd[3]!=0.0)ftot += x[12]+x[13]+x[14];


   if(ftot>1){
      stop_motors();
      _settextposition(9,47);
      printf("The object is in contact");
      break;
   }

   if(*panic==1)break;

   n++;

  }while(5);

  stop_motors();

}


void hold_obj(char *f, char *g, int *panic)

{

   int xh, x[15], ll, i, xmin[4];
   char cc;

   if(*g=='c'|| *g=='C'){xmin[0] = 185; xmin[1] = 20; xmin[2] = 45; xmin[3] = 55; }
   if(*g=='t'|| *g=='T'){xmin[0] = 145; xmin[1] = 10; xmin[2] = 45; xmin[3] = 155;
   if(*g=='k'|| *g=='K'){xmin[0] = 185; xmin[1] = 10; xmin[2] = 215; xmin[3] = 165;


   do{

      read_sensors(x);

      display(x);


      if(*f=='1'){ ll = 1; xh = 2;}
      if(*f=='2'){ ll = 2; xh = 4;}
      if(*f=='3'){ ll = 4; xh = 5;}
```

```
if( (x[4]<ll) && (x[5]<ll) && (x[0]>xmin[0]) ) outp(PC,0x1f);
else{
  if( (x[4]>xh) || (x[5]>xh) ) outp(PC,0x0f);
  else outp(PC,0x00);
}


dummy();


if( (x[6]<ll) && (x[7]<ll) && (x[8]<ll) && (x[1]>xmin[1])) outp(PC,0x3f);
else{
  if( (x[6]>xh) || (x[7]>xh) || (x[8]>xh) ) outp(PC,0x2f);
  else outp(PC,0x20);
}


dummy();


if( ( x[9] < ll) && (x[10] < ll) && (x[11] < ll) && (x[2]>xmin[2]) ) outp(PC,0
else{
  if( (x[9]>xh) || (x[10]>xh) || (x[11]>xh) ) outp(PC,0x4f);
  else outp(PC,0x40);
}


dummy();

if( (x[12]<ll) && (x[13]<ll) && (x[14]<ll) && (x[3]>xmin[3])) outp(PC,0x7f);
else{
  if( (x[12]>xh) || (x[13]>xh) || (x[14]>xh) ) outp(PC,0x6f);
  else outp(PC,0x60);
}


for(i=0;i<50;i++)dummy();

outp(PC,0x00);
dummy();
outp(PC,0x20);
dummy();
outp(PC,0x40);
dummy();
outp(PC,0x60);

if( x[0]<xmin[0] && x[1]<xmin[1] && x[2]<xmin[2] && x[3]<xmin[3]
&& (x[4]+ x[5]+ x[6]+ x[7]+ x[8]+ x[9]+ x[10]+ x[11]+ x[12]+ x[13]+ x[14]) <=
{
  _settextposition(9,47);
  printf("The object seems to have slipped");
}
}while(!kbhit());

cc = getch();

stop_motors();

}
```

A.4 Hand.c:

```
/*

   This pprogram was written to experiment with the hand. It prints
all of the senssor readings without calibration on the screen. It
allows the user to control the fingers with the keyboard. Each of the
motors have been assigned two keys. When the first key is pressed,
the corresponding motor receives full power in the forward direction
and when the second key is pressed the motor receives full power in
the reverse direction. If any other key is pressed, all of the motors
are stopped.

*/

#include <stdio.h>
#include <stdlib.h>
#include <bios.h>
#include <dos.h>
#include <time.h>
#include <graph.h>
#include <math.h>
#include <float.h>
#include <signal.h>
#include <conio.h>
#include <memory.h>


#define TRUE                           1
#define FALSE                          0


/*
Parallel Port Definations for our setup of the homebrew card It uses the Intel
8255 PIO chip PA, PB, PC are the programmable registers CO is the control
register. These are mapped into the I/O space of the PC
*/
#define IO_BASE_ADDR                   0x360
#define PA                             IO_BASE_ADDR
#define PB                             IO_BASE_ADDR+1
#define PC                             IO_BASE_ADDR+2
#define CO                             IO_BASE_ADDR+3
#define STOP_ALL                       18
#define SETUP_PIO                      0x90

void setupPioBoard(void);
void stop_motors(void);
void dummy(void);

main()
{
int x[8], y[8], z[8], i, j, p, n, out;
double t;
char inch;
```

```
clock_t start_t,end_t;

setupPioBoard();

stop_motors();

start_t = clock();

printf("\n\nThis program prints the sensed forces on the screen\n\n");

do  {

    n = n+1;

    for(i=0;i<8;i++){

        outp(PB, 120+i);

        for(j=0;j<70;j++);

        outp(PB, 96+i);

        for(j=0;j<70;j++);

        outp(PB, 104+i);

        for(j=0;j<70;j++);

        outp(PB, 24+i);

        for(j=0;j<70;j++);

        x[i] = inp(PA);

        for(j=0;j<70;j++);

        outp(PB, 56+i);

        for(j=0;j<70;j++);

        y[i] = inp(PA);

    }


    printf("%3d %3d %3d %3d    %3d %3d    %3d %3d ", x[0],x[1],x[2],x[3],x[4],x[5

    printf("%3d    %3d %3d %3d    %3d %3d     %3d\r", y[0],y[1],y[2],y[3],y[4],y[5

    if(kbhit())inch = getch();

    switch(inch){

        case 'q': case 'Q':  outp(PC, 0x0f); break;
```

```
         case 'a': case 'A':  outp(PC, 0x1f); break;

         case 'w': case 'W':  outp(PC, 0x2f); break;

         case 's': case 'S':  outp(PC, 0x3f); break;

         case 'e': case 'E':  outp(PC, 0x4f); break;

         case 'd': case 'D':  outp(PC, 0x5f); break;

         case 'r': case 'R':  outp(PC, 0x6f); break;

         case 'f': case 'F':  outp(PC, 0x7f); break;

         case 'z': case 'Z': exit(0); break;

         default:
           stop_motors();
           break;
      }

    } while(5);


  end_t = clock();

  t = ((double) (end_t - start_t))/n;

   printf("\n\nAverage time = %lf\n\n",t);

   stop_motors();
}


void setupPioBoard(void)
{
   outp(CO, SETUP_PIO);
   outp(PB, 0x78);
   outp(PC, 0x00);
}

void stop_motors(void)

{
    outp(PC, 0x00);
    dummy();
    outp(PC, 0x20);
    dummy();
    outp(PC, 0x40);
    dummy();
    outp(PC, 0x60);

}


void dummy()
{
   int a;
   for (a = 1; a < 50; a++);
}
```

APPENDIX B: THE MANUFACTURERS
DATA SHEETS

B.1 ADC 0809 A/D Converter:

ADC0808/ADC0809

National Semiconductor Corporation

ADC0808, ADC0809 8-Bit μP Compatible A/D Converters with 8-Channel Multiplexer

General Description

The ADC0808, ADC0809 data acquisition component is a monolithic CMOS device with an 8-bit analog-to-digital converter, 8-channel multiplexer and microprocessor compatible control logic. The 8-bit A/D converter uses successive approximation as the conversion technique. The converter features a high impedance chopper stabilized comparator, a 256R voltage divider with analog switch tree and a successive approximation register. The 8-channel multiplexer can directly access any of 8-single-ended analog signals.

The device eliminates the need for external zero and full-scale adjustments. Easy interfacing to microprocessors is provided by the latched and decoded multiplexer address inputs and latched TTL TRI-STATE® outputs.

The design of the ADC0808, ADC0809 has been optimized by incorporating the most desirable aspects of several A/D conversion techniques. The ADC0808, ADC0809 offers high speed, high accuracy, minimal temperature dependence, excellent long-term accuracy and repeatability, and consumes minimal power. These features make this device ideally suited to applications from process and machine control to consumer and automotive applications. For 16-channel multiplexer with common output (sample/hold port) see ADC0816 data sheet. (See AN-247 for more information.)

Features

- Easy interface to all microprocessors
- Operates ratiometrically or with 5 V_{DC} or analog span adjusted voltage reference
- No zero or full-scale adjust required
- 8-channel multiplexer with address logic
- 0V to 5V input range with single 5V power supply
- Outputs meet TTL voltage level specifications
- Standard hermetic or molded 28-pin DIP package
- 28-pin molded chip carrier package

Key Specifications

■ Resolution	8 Bits
■ Total Unadjusted Error	±½ LSB and ±1 LSB
■ Single Supply	5 V_{DC}
■ Low Power	15 mW
■ Conversion Time	100 μs

Block Diagram

TL/H/5672-1

See Ordering Information
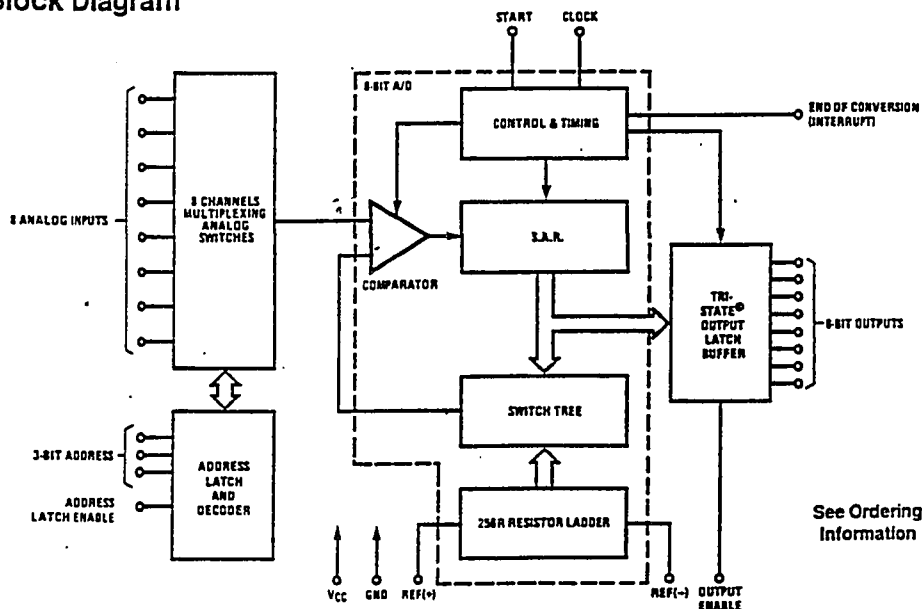
Absolute Maximum Ratings (Notes 1 & 2)

If Military/Aerospace specified devices are required, contact the National Semiconductor Sales Office/ Distributors for availability and specifications.

Supply Voltage (V_{CC}) (Note 3)	6.5V
Voltage at Any Pin Except Control Inputs	−0.3V to (V_{CC}+0.3V)
Voltage at Control Inputs (START, OE, CLOCK, ALE, ADD A, ADD B, ADD C)	−0.3V to +15V
Storage Temperature Range	−65°C to +150°C
Package Dissipation at T_A = 25°C	875 mW
Lead Temp. (Soldering, 10 seconds) Dual-In-Line Package (plastic) Dual-In-Line Package (ceramic) Molded Chip Carrier Package	 260°C 300°C
Vapor Phase (60 seconds)	215°C
Infrared (15 seconds)	220°C
ESD Susceptibility (Note 11)	400V

Operating Conditions (Notes 1 & 2)

Temperature Range (Note 1)	$T_{MIN} \le T_A \le T_{MAX}$
ADC0808CJ	−55°C≤T_A≤+125°C
ADC0808CCJ, ADC0808CCN, ADC0809CCN	−40°C≤T_A≤+85°C
ADC0808CCV, ADC0809CCV	−40°C ≤ T_A ≤ +85°C
Range of V_{CC} (Note 1)	4.5 V_{DC} to 6.0 V_{DC}

Electrical Characteristics

Converter Specifications: V_{CC} = 5 V_{DC} = $V_{REF(+)}$, $V_{REF(-)}$ = GND, $T_{MIN} \le T_A \le T_{MAX}$ and f_{CLK} = 640 kHz unless otherwise stated.

Symbol	Parameter	Conditions	Min	Typ	Max	Units
	ADC0808 Total Unadjusted Error (Note 5)	25°C T_{MIN} to T_{MAX}			±½ ±¾	LSB LSB
	ADC0809 Total Unadjusted Error (Note 5)	0°C to 70°C T_{MIN} to T_{MAX}			±1 ±1¼	LSB LSB
	Input Resistance	From Ref(+) to Ref(−)	1.0	2.5		kΩ
	Analog Input Voltage Range	(Note 4) V(+) or V(−)	GND−0.10		V_{CC}+0.10	V_{DC}
$V_{REF(+)}$	Voltage, Top of Ladder	Measured at Ref(+)		V_{CC}	V_{CC}+0.1	V
$\dfrac{V_{REF(+)} + V_{REF(-)}}{2}$	Voltage, Center of Ladder		V_{CC}/2−0.1	V_{CC}/2	V_{CC}/2+0.1	V
$V_{REF(-)}$	Voltage, Bottom of Ladder	Measured at Ref(−)	−0.1	0		V
I_{IN}	Comparator Input Current	f_c = 640 kHz, (Note 6)	−2	±0.5	2	μA

Electrical Characteristics

Digital Levels and DC Specifications: ADC0808CJ 4.5V≤V_{CC}≤5.5V, −55°C≤T_A≤+125°C unless otherwise noted ADC0808CCJ, ADC0808CCN, ADC0808CCV, ADC0809CCN and ADC0809CCV, 4.75≤V_{CC}≤5.25V, −40°C≤T_A≤+85°C unless otherwise noted

Symbol	Parameter	Conditions	Min	Typ	Max	Units
ANALOG MULTIPLEXER						
$I_{OFF(+)}$	OFF Channel Leakage Current	V_{CC}=5V, V_{IN}=5V, T_A=25°C T_{MIN} to T_{MAX}		10	200 1.0	nA μA
$I_{OFF(-)}$	OFF Channel Leakage Current	V_{CC}=5V, V_{IN}=0, T_A=25°C T_{MIN} to T_{MAX}	−200 −1.0	−10		nA μA

Functional Description (Continued)

The A/D converter's successive approximation register (SAR) is reset on the positive edge of the start conversion (SC) pulse. The conversion is begun on the falling edge of the start conversion pulse. A conversion in process will be interrupted by receipt of a new start conversion pulse. Continuous conversion may be accomplished by tying the end-of-conversion (EOC) output to the SC input. If used in this mode, an external start conversion pulse should be applied after power up. End-of-conversion will go low between 0 and 8 clock pulses after the rising edge of start conversion.

The most important section of the A/D converter is the comparator. It is this section which is responsible for the ultimate accuracy of the entire converter. It is also the comparator drift which has the greatest influence on the repeatability of the device. A chopper-stabilized comparator provides the most effective method of satisfying all the converter requirements.

The chopper-stabilized comparator converts the DC input signal into an AC signal. This signal is then fed throught a high gain AC amplifier and has the DC level restored. This technique limits the drift component of the amplifier since the drift is a DC component which is not passed by the AC amplifier. This makes the entire A/D converter extremely insensitive to temperature, long term drift and input offset errors.

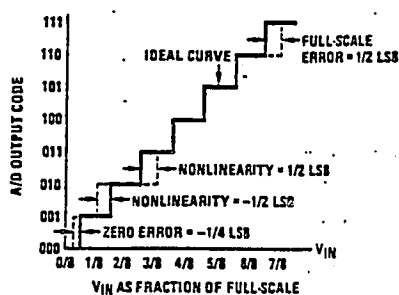*Figure 4* shows a typical error curve for the ADC0808 as measured using the procedures outlined in AN-179.

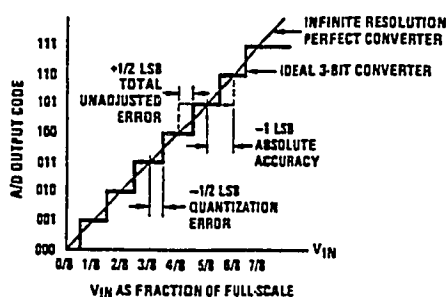FIGURE 2. 3-Bit A/D Transfer Curve

FIGURE 3. 3-Bit A/D Absolute Accuracy Curve
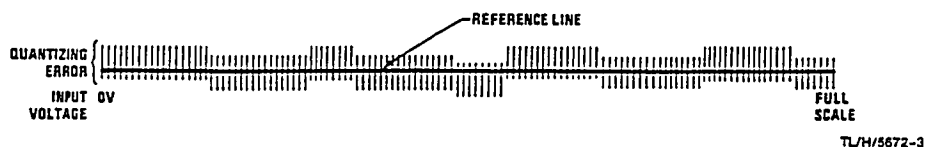
FIGURE 4. Typical Error Curve

TL/H/5672-3

Electrical Characteristics (Continued)

Digital Levels and DC Specifications: ADC0808CJ $4.5V \leq V_{CC} \leq 5.5V$, $-55°C \leq T_A \leq +125°C$ unless otherwise noted ADC0808CCJ, ADC0808CCN, ADC0808CCV, ADC0809CCN and ADC0809CCV, $4.75 \leq V_{CC} \leq 5.25V$, $-40°C \leq T_A \leq +85°C$ unless otherwise noted

Symbol	Parameter	Conditions	Min	Typ	Max	Units
CONTROL INPUTS						-
$V_{IN(1)}$	Logical "1" Input Voltage		$V_{CC}-1.5$			V
$V_{IN(0)}$	Logical "0" Input Voltage				1.5	V
$I_{IN(1)}$	Logical "1" Input Current (The Control Inputs)	$V_{IN}=15V$			1.0	μA
$I_{IN(0)}$	Logical "0" Input Current (The Control Inputs)	$V_{IN}=0$		-1.0		μA
I_{CC}	Supply Current	$f_{CLK}=640$ kHz		0.3	3.0	mA
DATA OUTPUTS AND EOC (INTERRUPT)						
$V_{OUT(1)}$	Logical "1" Output Voltage	$I_O=-360\,\mu A$	$V_{CC}-0.4$			V
$V_{OUT(0)}$	Logical "0" Output Voltage	$I_O=1.6$ mA			0.45	V
$V_{OUT(0)}$	Logical "0" Output Voltage EOC	$I_O=1.2$ mA			0.45	V
I_{OUT}	TRI-STATE Output Current	$V_O=5V$ $V_O=0$	-3		3	μA μA

Electrical Characteristics

Timing Specifications $V_{CC}=V_{REF(+)}=5V$, $V_{REF(-)}=GND$, $t_r=t_f=20$ ns and $T_A=25°C$ unless otherwise noted.

Symbol	Parameter	Conditions	Min	Typ	Max	Units
t_{WS}	Minimum Start Pulse Width	(Figure 5)		100	200	ns
t_{WALE}	Minimum ALE Pulse Width	(Figure 5)		100	200	ns
t_s	Minimum Address Set-Up Time	(Figure 5)		25	50	ns
t_H	Minimum Address Hold Time	(Figure 5)		25	50	ns
t_D	Analog MUX Delay Time From ALE	$R_S=0\Omega$ (Figure 5)		1	2.5	μS
t_{H1}, t_{H0}	OE Control to Q Logic State	$C_L=50$ pF, $R_L=10k$ (Figure 8)		125	250	ns
t_{1H}, t_{0H}	OE Control to Hi-Z	$C_L=10$ pF, $R_L=10k$ (Figure 8)		125	250	ns
t_C	Conversion Time	$f_C=640$ kHz, (Figure 5) (Note 7)	90	100	116	μS
f_C	Clock Frequency		10	640	1280	kHz
t_{EOC}	EOC Delay Time	(Figure 5)	0		$8+2\,\mu S$	Clock Periods
C_{IN}	Input Capacitance	At Control Inputs		10	15	pF
C_{OUT}	TRI-STATE Output Capacitance	At TRI-STATE Outputs, (Note 12)		10	15	pF

Note 1: Absolute Maximum Ratings indicate limits beyond which damage to the device may occur. DC and AC electrical specifications do not apply when operating the device beyond its specified operating conditions.

Note 2: All voltages are measured with respect to GND, unless otherwise specified.

Note 3: A zener diode exists, internally, from V_{CC} to GND and has a typical breakdown voltage of 7 V_{DC}.

Note 4: Two on-chip diodes are tied to each analog input which will forward conduct for analog input voltages one diode drop below ground or one diode drop greater than the V_{CC} supply. The spec allows 100 mV forward bias of either diode. This means that as long as the analog V_{IN} does not exceed the supply voltage by more than 100 mV, the output code will be correct. To achieve an absolute $0V_{DC}$ to $5V_{DC}$ input voltage range will therefore require a minimum supply voltage of 4.900 V_{DC} over temperature variations, initial tolerance and loading.

Note 5: Total unadjusted error includes offset, full-scale, linearity, and multiplexer errors. See Figure 3. None of these A/Ds requires a zero or full-scale adjust. However, if an all zero code is desired for an analog input other than 0.0V, or if a narrow full-scale span exists (for example: 0.5V to 4.5V full-scale) the reference voltages can be adjusted to achieve this. See Figure 13.

Note 6: Comparator input current is a bias current into or out of the chopper stabilized comparator. The bias current varies directly with clock frequency and has little temperature dependence (Figure 6). See paragraph 4.0.

Note 7: The outputs of the data register are updated one clock cycle before the rising edge of EOC.

Note 8: Human body model, 100 pF discharged through a 1.5 kΩ resistor.

Functional Description

Multiplexer. The device contains an 8-channel single-ended analog signal multiplexer. A particular input channel is selected by using the address decoder. Table I shows the input states for the address lines to select any channel. The address is latched into the decoder on the low-to-high transition of the address latch enable signal.

TABLE I

SELECTED	ADDRESS LINE		
ANALOG CHANNEL	C	B	A
IN0	L	L	L
IN1	L	L	H
IN2	L	H	L
IN3	L	H	H
IN4	H	L	L
IN5	H	L	H
IN6	H	H	L
IN7	H	H	H

CONVERTER CHARACTERISTICS

The Converter

The heart of this single chip data acquisition system is its 8-bit analog-to-digital converter. The converter is designed to give fast, accurate, and repeatable conversions over a wide range of temperatures. The converter is partitioned into 3 major sections: the 256R ladder network, the successive approximation register, and the comparator. The converter's digital outputs are positive true.

The 256R ladder network approach (Figure 1) was chosen over the conventional R/2R ladder because of its inherent monotonicity, which guarantees no missing digital codes. Monotonicity is particularly important in closed loop feedback control systems. A non-monotonic relationship can cause oscillations that will be catastrophic for the system. Additionally, the 256R network does not cause load variations on the reference voltage.

The bottom resistor and the top resistor of the ladder network in Figure 1 are not the same value as the remainder of the network. The difference in these resistors causes the output characteristic to be symmetrical with the zero and full-scale points of the transfer curve. The first output transition occurs when the analog signal has reached $+\frac{1}{2}$ LSB and succeeding output transitions occur every 1 LSB later up to full-scale.

The successive approximation register (SAR) performs 8 iterations to approximate the input voltage. For any SAR type converter, n-iterations are required for an n-bit converter. Figure 2 shows a typical example of a 3-bit converter. In the ADC0808, ADC0809, the approximation technique is extended to 8 bits using the 256R network.
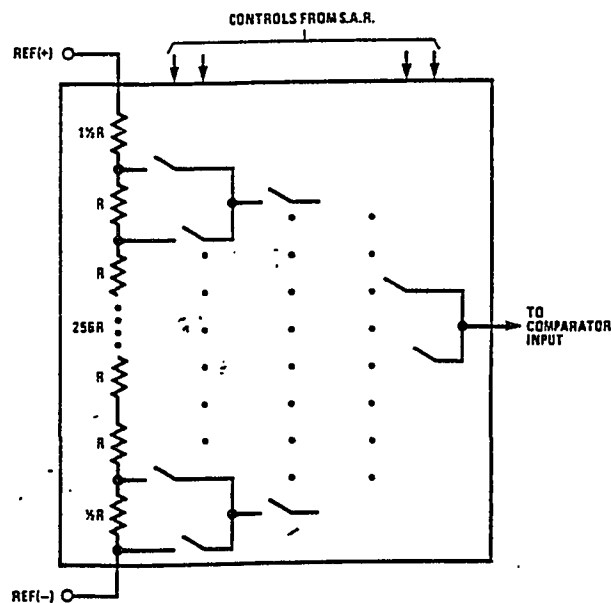
FIGURE 1. Resistor Ladder and Switch Tree

TL/H/5672-2

B.2 Lm 324 Operational Amplifier:

National Semiconductor

LM124/LM224/LM324, LM124A/LM224A/LM324A, LM2902 Low Power Quad Operational Amplifiers

General Description

The LM124 series consists of four independent, high gain, internally frequency compensated operational amplifiers which were designed specifically to operate from a single power supply over a wide range of voltages. Operation from split power supplies is also possible and the low power supply current drain is independent of the magnitude of the power supply voltage.

Application areas include transducer amplifiers, DC gain blocks and all the conventional op amp circuits which now can be more easily implemented in single power supply systems. For example, the LM124 series can be directly operated off of the standard +5 V_{DC} power supply voltage which is used in digital systems and will easily provide the required interface electronics without requiring the additional ±15 V_{DC} power supplies.

Unique Characteristics

- In the linear mode the input common-mode voltage range includes ground and the output voltage can also swing to ground, even though operated from only a single power supply voltage.
- The unity gain cross frequency is temperature compensated.
- The input bias current is also temperature compensated.

Advantages

- Eliminates need for dual supplies
- Four internally compensated op amps in a single package
- Allows directly sensing near GND and V_{OUT} also goes to GND
- Compatible with all forms of logic
- Power drain suitable for battery operation

Features

- Internally frequency compensated for unity gain
- Large DC voltage gain   100 dB
- Wide bandwidth (unity gain)   1 MHz (temperature compensated)
- Wide power supply range:
  Single supply   3 V_{DC} to 32 V_{DC}
  or dual supplies   ±1.5 V_{DC} to ±16 V_{DC}
- Very low supply current drain (700 μA)—essentially independent of supply voltage
- Low input biasing current   45 nA_{DC} (temperature compensated)
- Low input offset voltage   2 mV_{DC} and offset current   5 nA_{DC}
- Input common-mode voltage range includes ground
- Differential input voltage range equal to the power supply voltage
- Large output voltage swing   0 V_{DC} to V$^+$ − 1.5 V_{DC}

Connection Diagram

Dual-In-Line Package

Top View

TL/H/9299–1
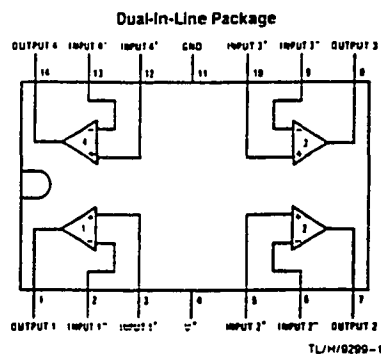
Order Number LM124J, LM124AJ, LM224J,
LM224AJ, LM324J, LM324AJ, LM324M, LM324AM,
LM2902M, LM324N, LM324AN or LM2902N
See NS Package Number J14A, M14A or N14A

Schematic Diagram (Each Amplifier)

TL/H/9299–2

LM124/LM224/LM324/LM124A/LM224A/LM324A/LM2902

Absolute Maximum Ratings

If Military/Aerospace specified devices are required, please contact the National Semiconductor Sales Office/Distributors for availability and specifications. (Note 9)

	LM124/LM224/LM324 LM124A/LM224A/LM324A	LM2902
Supply Voltage, V⁺	32 V_DC or ± 16 V_DC	26 V_DC or ± 13 V_DC
Differential Input Voltage	32 V_DC	26 V_DC
Input Voltage	−0.3 V_DC to +32 V_DC	−0.3 V_DC to +26 V_DC
Input Current (V_IN < −0.3 V_DC) (Note 3)	50 mA	50 mA
Power Dissipation (Note 1)		
Molded DIP	1130 mW	1130 mW
Cavity DIP	1260 mW	1260 mW
Small Outline Package	800 mW	800 mW
Output Short-Circuit to GND (One Amplifier) (Note 2) V⁺ ≤ 15 V_DC and T_A = 25°C	Continuous	Continuous
Operating Temperature Range		−40°C to +85°C
LM324/LM324A	0°C to +70°C	
LM224/LM224A	−25°C to +85°C	
LM124/LM124A	−55°C to +125°C	

	LM124/LM224A/LM124A/LM224A/LM324A	LM2902
Storage Temperature Range	−65°C to +150°C	−65°C to +150°C
Lead Temperature (Soldering, 10 seconds)	260°C	260°C
Soldering Information		
Dual-In-Line Package		
Soldering (10 seconds)	260°C	260°C
Small Outline Package		
Vapor Phase (60 seconds)	215°C	215°C
Infrared (15 seconds)	220°C	220°C

See AN-450 "Surface Mounting Methods and Their Effect on Product Reliability" for other methods of soldering surface mount devices.

ESD Tolerance (Note 10) 250V 250V

Electrical Characteristics V⁺ = +5.0 V_DC (Note 4), unless otherwise stated

Parameter	Conditions	LM124A			LM224A			LM324A			LM124/LM224			LM124A/LM224A/LM324 LM124A/LM224A/LM324A			LM2902			Units
		Min	Typ	Max	Min	Typ	Max	Min	Typ	Max	Min	Typ	Max	Min	Typ	Max	Min	Typ	Max	
Input Offset Voltage	(Note 5) T_A = 25°C		±1	±2		±1	±3		±2	±3		±2	±5		±2	±7		±2	±7	mV_DC
Input Bias Current (Note 6)	I_IN(+) or I_IN(−), V_CM = 0V, T_A = 25°C		20	50		40	80		45	100		45	150		45	250		45	250	nA_DC
Input Offset Current	I_IN(+) − I_IN(−), V_CM = 0V, T_A = 25°C		±2	±10		±2	±15		±5	±30		±3	±30		±5	±50		±5	±50	nA_DC
Input Common-Mode Voltage Range (Note 7)	V⁺ = 30 V_DC, (LM2902, V⁺ = 26 V_DC), T_A = 25°C	0		V⁺−1.5	0		V⁺−1.5	0		V⁺−1.5	0		V⁺−1.5	0		V⁺−1.5	0		V⁺−1.5	V_DC
Supply Current	Over Full Temperature Range R_L = ∞ On All Op Amps																			mA_DC
	V⁺ = 30V (LM2902 V⁺ = 26V)		1.5	3		1.5	3		1.5	3		1.5	3		1.5	3		1.5	3	
	V⁺ = 5V		0.7	1.2		0.7	1.2		0.7	1.2		0.7	1.2		0.7	1.2		0.7	1.2	
Large Signal Voltage Gain	V⁺ = 15 V_DC, R_L ≥ 2 kΩ, (V_O = 1 V_DC to 11 V_DC), T_A = 25°C	50	100		50	100		25	100		50	100		25	100		25	100		V/mV
Common-Mode Rejection Ratio	DC, V_CM = 0V to V⁺ −1.5 V_DC, T_A = 25°C	70	85		70	85		65	85		70	85		65	85		50	70		dB
Power Supply Rejection Ratio	DC, V⁺ = 5 V_DC to 30 V_DC (LM2902, V⁺ = 5 V_DC to 26 V_DC), T_A = 25°C	65	100		65	100		65	100		65	100		65	100		50	100		dB

Electrical Characteristics V⁺ = +50 VDC (Note 4) unless otherwise stated (Continued)

Parameter	Conditions	LM124A Min	Typ	Max	LM224A Min	Typ	Max	LM324A Min	Typ	Max	LM124/LM224 Min	Typ	Max	LM324 Min	Typ	Max	LM2902 Min	Typ	Max	Units
Amplifier-to-Amplifier Coupling (Note 6)	f = 1 kHz to 20 kHz, T_A = 25°C (Input Referred)		-120			-120			-120			-120			-120			-120		dB
Output Current Source	V_{IN}^+ = 1 V_{DC}, V_{IN}^- = 0 V_{DC}, V^+ = 15 V_{DC}, V_O = 2 V_{DC}, T_A = 25°C	20	40		20	40		20	40		20	40		20	40		20	40		mA_{DC}
Sink	V_{IN}^- = 1 V_{DC}, V_{IN}^+ = 0 V_{DC}, V^+ = 15 V_{DC}, V_O = 2 V_{DC}, T_A = 25°C	10	20		10	20		10	20		10	20		10	20		10	20		mA_{DC}
	V_{IN}^- = 1 V_{DC}, V_{IN}^+ = 0 V_{DC}, V^+ = 15 V_{DC}, V_O = 200 mV_{DC}, T_A = 25°C	12	50		12	50		12	50		12	50		12	50		12	50		μA_{DC}
Short Circuit to Ground	(Note 2) V^+ = 15 V_{DC}, T_A = 25°C		40	60		40	60		40	60		40	60		40	60		40	60	mA_{DC}
Input Offset Voltage	(Note 5)			±4			±4			±5			±7			±9			±10	mV_{DC}
Input Offset Voltage Drift	R_S = 0Ω		±7	±20		±7	±20		±7	±30		±7			±7			±7		$\mu V/°C$
Input Offset Current	$I_{IN(+)}$ − $I_{IN(-)}$, V_{CM} = 0V			±30			±30			±75			±100			±150		±45	±200	nA_{DC}
Input Offset Current Drift	R_S = 0Ω		±10	±200		±10	±200		±10	±200		±10			±10			±10		$pA_{DC}/°C$
Input Bias Current	$I_{IN(+)}$ or $I_{IN(-)}$		40	100		40	100		40	200		40	300		40	500		40	500	nA_{DC}
Input Common-Mode Voltage Range (Note 7)	V^+ = +30 V_{DC} (LM2902, V^+ = 26 V_{DC})	0		V^+−2	0		V^+−2	0		V^+−2	0		V^+−2	0		V^+−2	0		V^+−2	V_{DC}
Large Signal Voltage Gain	V^+ = +15 V_{DC} (V_O Swing = 1 V_{DC} to 11 V_{DC}) R_L ≥ 2 kΩ		25			25			15			25			15			15		V/mV
Output Voltage V_{OH}	V^+ = +30 V_{DC}, R_L = 2 kΩ		26			26			26			26			26			22		V_{DC}
Swing	R_L ≥ 10 kΩ (LM2902, V^+ = 26 V_{DC})	27	28		27	28		27	28		27	28		27	28		23	24		V_{DC}
V_{OL}	V^+ = 5 V_{DC}, R_L ≤ 10 kΩ		5	20		5	20		5	20		5	20		5	20		5	100	mV_{DC}

LM124/LM224/LM324/LM124A/LM224A/LM324A/LM2902

Electrical Characteristics $v^+ = +5.0$ Vdc (Note 4) unless otherwise stated (Continued)

Parameter		Conditions	LM124A			LM224A			LM324A			LM124/LM224			LM324			LM2902			Units
			Min	Typ	Max	Min	Typ	Max	Min	Typ	Max	Min	Typ	Max	Min	Typ	Max	Min	Typ	Max	
Output Current	Source	$V_O = 2$ Vdc, $V_{IN}^+ = +1$ Vdc, $V_{IN}^- = 0$ Vdc, $V^+ = 15$ Vdc	10	20		10	20		10	20		10	20		10	20		10	20		mAdc
	Sink	$V_{IN}^- = +1$ Vdc, $V_{IN}^+ = 0$ Vdc, $V^+ = 15$ Vdc	10	15		5	8		5	8		5	8		5	8		5	8		

Note 1: For operating at high temperatures, the LM324/LM324A, LM2902 must be derated based on a +125°C maximum junction temperature and a thermal resistance of 88°C/W which applies for the device soldered in a printed circuit board, operating in a still air ambient. The LM224/LM224A and LM124/LM124A can be derated based on a +150°C maximum junction temperature. The dissipation is the total of all four amplifiers—use external resistors, where possible, to allow the amplifier to saturate or to reduce the power which is dissipated in the integrated circuit.

Note 2: Short circuits from the output to V^+ can cause excessive heating and eventual destruction. When considering short circuits to ground, the maximum output current is approximately 40 mA independent of the magnitude of V^+. At values of supply voltage in excess of +15 Vpc continuous short-circuits can exceed the power dissipation ratings and cause eventual destruction. Destructive dissipation can result from simultaneous shorts on all amplifiers.

Note 3: This input current will only exist when the voltage at any of the input leads is driven negative. It is due to the collector-base junction of the input PNP transistors becoming forward biased and thereby acting as input diode clamps. In addition to this diode action, there is also lateral NPN parasitic transistor action on the IC chip. This transistor action can cause the output voltages of the op amps to go to the V^+ voltage level (or to ground for a large overdrive) for the time duration that an input is driven negative. This is not destructive and normal output states will re-establish when the input voltage, which was negative, again returns to a value greater than -0.3 Vdc (at 25°C).

Note 4: These specifications are limited to $-55°C \leq T_A \leq +125°C$ for the LM124/LM124A. With the LM224/LM224A, at temperature specifications are limited to $-25°C \leq T_A \leq +85°C$, the LM124/LM124A temperature specifications are limited to 0°C $\leq T_A \leq +70°C$, and the LM2902 specifications are limited to $-40°C \leq T_A \leq +85°C$.

Note 5: $V_O = 1.4$ Vdc, $R_S = 0\Omega$ with V^+ from 5 Vdc to 30 Vdc; and over the full input common-mode range (0 Vdc to $V^+ - 1.5$ Vdc) at 25°C; for LM2902, V^+ from 5 Vdc to 26 Vdc.

Note 6: The direction of the input current is out of the IC due to the PNP input stage. This current is essentially constant, independent of the state of the output so no loading change exists on the input lines.

Note 7: The input common-mode voltage of either input signal voltage should not be allowed to go negative by more than 0.3V (at 25°C). The upper end of the common-mode voltage range is $V^+ - 1.5$V (at 25°C), but either or both inputs can go to +32 Vdc without damage (+26 Vdc for LM2902), independent of the magnitude of V^+.

Note 8: Due to proximity of external components, insure that coupling is not originating via stray capacitance between these external parts. This typically can be detected as this type of capacitance increases at higher frequencies.

Note 9: Refer to RETS124X for LM124A military specifications and refer to RETS124X for LM124 military specifications.

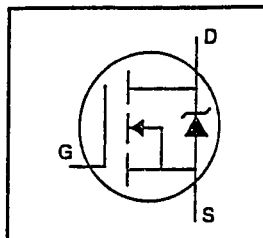Note 10: Human body model. 1.5 kΩ in series with 100 pF.

B.3 Field Effect Transistors:

international IOR Rectifier

IRFD1Z0

HEXFET® Power MOSFET

• Dynamic dv/dt Rating
• Repetitive Avalanche Rated
• For Automatic Insertion
• End Stackable
• 175°C Operating Temperature
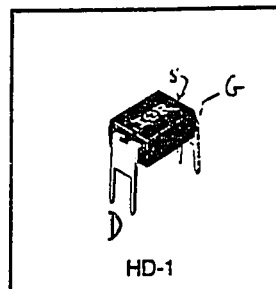• Fast Switching
• Ease of Paralleling

$V_{DSS} = 100V$

$R_{DS(on)} = 2.4\Omega$

$I_D = 0.50A$

Description

Third Generation HEXFETs from International Rectifier provide the designer with the best combination of fast switching, ruggedized device design, low on-resistance and cost-effectiveness.

The 4-pin DIP package is a low cost machine-insertable case style which can be stacked in multiple combinations on standard 0.1 inch pin centers. The dual drain serves as a thermal link to the mounting surface for power dissipation levels up to 1 watt.

HD-1

Absolute Maximum Ratings

	Parameter	Max.	Units
I_D @ $T_C = 25°C$	Continuous Drain Current, V_{GS} @ 10 V	0.50	A
I_D @ $T_C = 100°C$	Continuous Drain Current, V_{GS} @ 10 V	0.36	
I_{DM}	Pulsed Drain Current ①	4.0	
P_D @ $T_C = 25°C$	Power Dissipation	1.3	W
	Linear Derating Factor	0.10	W/°C
V_{GS}	Gate-to-Source Voltage	±20	V
E_{AS}	Single Pulse Avalanche Energy ②	9.8	mJ
I_{AR}	Avalanche Current ①	0.50	A
E_{AR}	Repetitive Avalanche Energy ①	0.13	mJ
dv/dt	Peak Diode Recovery dv/dt ③	5.5	V/ns
T_J T_{STG}	Operating Junction and Storage Temperature Range	-55 to +175	°C
	Soldering Temperature, for 10 seconds	300 (1.6mm from case)	

Thermal Resistance

	Parameter	Min.	Typ.	Max.	Units
$R_{\theta JA}$	Junction-to-Ambient	—	—	120	°C/W

International IIR Rectifier

IRFD9110

HEXFET® Power MOSFET

- Dynamic dv/dt Rating
- Repetitive Avalanche Rated
- For Automatic Insertion
- End Stackable
- P-Channel
- 175°C Operating Temperature
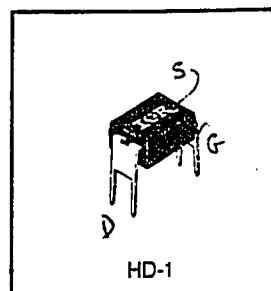- Fast Switching
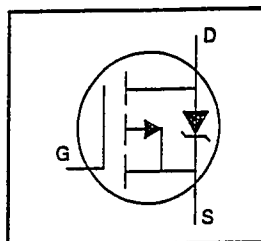
$V_{DSS} = -100V$

$R_{DS(on)} = 1.2\Omega$

$I_D = -0.70A$

Description

Third Generation HEXFETs from International Rectifier provide the designer with the best combination of fast switching, ruggedized device design, low on-resistance and cost-effectiveness.

The 4-pin DIP package is a low cost machine-insertable case style which can be stacked in multiple combinations on standard 0.1 inch pin centers. The dual drain serves as a thermal link to the mounting surface for power dissipation levels up to 1 watt.

HD-1

Absolute Maximum Ratings

	Parameter	Max.	Units
I_D @ $T_C = 25°C$	Continuous Drain Current, V_{GS} @ -10 V	-0.70	A
I_D @ $T_C = 100°C$	Continuous Drain Current, V_{GS} @ -10 V	-0.49	
I_{DM}	Pulsed Drain Current ①	-5.6	
P_D @ $T_C = 25°C$	Power Dissipation	1.3	W
	Linear Derating Factor	0.0083	W/°C
V_{GS}	Gate-to-Source Voltage	±20	V
E_{AS}	Single Pulse Avalanche Energy ②	140	mJ
I_{AR}	Avalanche Current ①	-0.70	A
E_{AR}	Repetitive Avalanche Energy ①	0.13	mJ
dv/dt	Peak Diode Recovery dv/dt ③	-5.5	V/ns
T_J T_{STG}	Operating Junction and Storage Temperature Range	-55 to +175	°C
	Soldering Temperature, for 10 seconds	300 (1.6mm from case)	

Thermal Resistance

	Parameter	Min.	Typ.	Max.	Units
$R_{θJA}$	Junction-to-Ambient	—	—	120	°C/W

JRFD1Z0

IɎR

Electrical Characteristics @ TJ = 25°C (unless otherwise specified)

	Parameter	Min.	Typ.	Max.	Units	Test Conditions
$V_{(BR)DSS}$	Drain-to-Source Breakdown Voltage	100	—	—	V	$V_{GS}=0V$, $I_D=250\mu A$
$\Delta V_{(BR)DSS}/\Delta T_J$	Breakdown Voltage Temp. Coefficient	—	0.12	—	V/°C	Reference to 25°C, $I_D=1mA$
$R_{DS(on)}$	Static Drain-to-Source On-Resistance	—	—	2.4	Ω	$V_{GS}=10V$, $I_D=0.30A$ ④
$V_{GS(th)}$	Gate Threshold Voltage	2.0	—	4.0	V	$V_{DS}=V_{GS}$, $I_D=250\mu A$
g_{fs}	Forward Transconductance	1.6	—	—	S	$V_{DS}=50V$, $I_D=0.30A$ ④
I_{DSS}	Drain-to-Source Leakage Current	—	—	25	μA	$V_{DS}=100V$, $V_{GS}=0V$
		—	—	250		$V_{DS}=80V$, $V_{GS}=0V$, $T_J=150°C$
I_{GSS}	Gate-to-Source Forward Leakage	—	—	100	nA	$V_{GS}=20V$
	Gate-to-Source Reverse Leakage	—	—	-100		$V_{GS}=-20V$
Q_g	Total Gate Charge	—	—	1.6	nC	$I_D=0.90A$
Q_{gs}	Gate-to-Source Charge	—	—	0.68		$V_{DS}=80V$
Q_{gd}	Gate-to-Drain ("Miller") Charge	—	—	0.95		$V_{GS}=10V$ See Fig. 6 and 13 ④
$t_{d(on)}$	Turn-On Delay Time	—	7.8	—	ns	$V_{DD}=50V$
t_r	Rise Time	—	4.5	—		$I_D=0.90A$
$t_{d(off)}$	Turn-Off Delay Time	—	11	—		$R_G=50\Omega$
t_f	Fall Time	—	4.7	—		$R_D=55\Omega$ See Figure 10 ④
L_D	Internal Drain Inductance	—	4.0	—	nH	Between lead, 6 mm (0.25in.) from package and center of die contact
L_S	Internal Source Inductance	—	6.0	—		
C_{iss}	Input Capacitance	—	39	—	pF	$V_{GS}=0V$
C_{oss}	Output Capacitance	—	18	—		$V_{DS}=25V$
C_{rss}	Reverse Transfer Capacitance	—	2.8	—		$f=1.0MHz$ See Figure 5

Source-Drain Ratings and Characteristics

	Parameter	Min.	Typ.	Max.	Units	Test Conditions
I_S	Continuous Source Current (Body Diode)	—	—	0.50	A	MOSFET symbol showing the integral reverse p-n junction diode.
I_{SM}	Pulsed Source Current (Body Diode) ①	—	—	4.0		
V_{SD}	Diode Forward Voltage	—	—	1.4	V	$T_J=25°C$, $I_S=0.50A$, $V_{GS}=0V$ ④
t_{rr}	Reverse Recovery Time	—	57	71	ns	$T_J=25°C$, $I_F=0.90A$
Q_{rr}	Reverse Recovery Charge	—	0.27	0.41	μC	di/dt=100A/μs ④
t_{on}	Forward Turn-On Time	Intrinsic turn-on time is negligible (turn-on is dominated by Ls+Lo)				

Notes:
① Repetitive rating; pulse width limited by max. junction temperature (See Figure 11)

② $V_{DD}=25V$, starting $T_J=25°C$, L=14mH $R_G=25\Omega$, $I_{AS}=1.0A$ (See Figure 12)

③ $I_{SD}≤0.50A$, di/dt≤25A/μs, $V_{DD}≤V_{(BR)DSS}$, $T_J≤175°C$

④ Pulse width ≤ 300 μs; duty cycle ≤2%.

IRFD9110

Electrical Characteristics @ TJ = 25°C (unless otherwise specified)

	Parameter	Min.	Typ.	Max.	Units	Test Conditions
V(BR)DSS	Drain-to-Source Breakdown Voltage	-100	—	—	V	VGS=0V, ID=-250µA
∆V(BR)DSS/∆TJ	Breakdown Voltage Temp. Coefficient	—	-0.091	—	V/°C	Reference to 25°C, ID=-1mA
RDS(on)	Static Drain-to-Source On-Resistance	—	—	1.2	Ω	VGS=-10V, ID=-0.42A ④
VGS(th)	Gate Threshold Voltage	-2.0	—	-4.0	V	VDS=VGS, ID=-250µA
gfs	Forward Transconductance	0.60	—	—	S	VDS=-50V, ID=-0.42A ④
IDSS	Drain-to-Source Leakage Current	—	—	-100	µA	VDS=-100V, VGS=0V
		—	—	-500		VDS=-80V, VGS=0V, TJ=150°C
IGSS	Gate-to-Source Forward Leakage	—	—	-100	nA	VGS=-20V
	Gate-to-Source Reverse Leakage	—	—	100		VGS=20V
Qg	Total Gate Charge	—	—	8.7	nC	ID=-4.0A
Qgs	Gate-to-Source Charge	—	—	2.2		VDS=-80V
Qgd	Gate-to-Drain ("Miller") Charge	—	—	4.1		VGS=-10V See Fig. 6 and 13 ④
td(on)	Turn-On Delay Time	—	10	—	ns	VDD=-50V
tr	Rise Time	—	27	—		ID=-4.0A
td(off)	Turn-Off Delay Time	—	15	—		RG=24Ω
tf	Fall Time	—	17	—		RD=11Ω See Figure 10 ④
LD	Internal Drain Inductance	—	4.0	—	nH	Between lead, 6 mm (0.25in.) from package and center of die contact
LS	Internal Source Inductance	—	6.0	—		
Ciss	Input Capacitance	—	200	—	pF	VGS=0V
Coss	Output Capacitance	—	94	—		VDS=-25V
Crss	Reverse Transfer Capacitance	—	18	—		f=1.0MHz See Figure 5

Source-Drain Ratings and Characteristics

	Parameter	Min.	Typ.	Max.	Units	Test Conditions
IS	Continuous Source Current (Body Diode)	—	—	-0.70	A	MOSFET symbol showing the integral reverse p-n junction diode.
ISM	Pulsed Source Current (Body Diode) ①	—	—	-5.6		
VSD	Diode Forward Voltage	—	—	-5.5	V	TJ=25°C, IS=-0.70A, VGS=0V ④
trr	Reverse Recovery Time	—	82	160	ns	TJ=25°C, IF=-4.0A
Qrr	Reverse Recovery Charge	—	0.15	0.30	µC	di/dt=100A/µs ④

Notes:

① Repetitive rating; pulse width limited by max. junction temperature (See Figure 11)

② VDD=-25V, starting TJ=25°C, L=52mH RG=25Ω, IAS=-2.0A (See Figure 12)

③ ISD≤-4.0A, di/dt≤75A/µs, VDD≤V(BR)DSS, TJ≤175°C
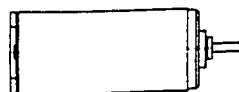
④ Pulse width ≤ 300 µs; duty cycle ≤2%.

B.4 The Motors:

MicroMo® MOTORS

DC MicroMotors Series 1331

- ▣ 1-oz.-in Stall Torque
- ▣ Samarium Cobalt Magnet
- ▣ Fits Our 15/5 Series Heavy Duty Gearhead
- ▣ Reinforced Brushes Standard
- ▣ Available with integral magnetic encoder
  (15 or 16 pulses per rev)

Actual Size

Continuous Duty Ratings:

Speeds up to 12,000 RPM
Torque up to .35 oz-in.
Output Power up to 2 Watts

Electrical Specifications: @ 72°F (22°C)

For Motor Type 1331T	4.5S	006S	012S	024S
Supply Voltage nom. (Volts)	4.5	6	12	24
Armature Resistance (Ohm)±12%	2.2	3.6	13.3	55
Max. Power Output (Watts)[1]	2.3	2.5	2.7	2.6
Max. Efficiency (%)[1]	75	77	76	75
No Load Speed (RPM) ±12[1]	10,800	10,900	11,300	11,400
No Load Current (mA) ±50%[2]	35	25	15	8
Friction Torque (@ No Load Speed)(oz-in)	.020	.018	.021	.023
Velocity Constant (RPM/Volt)	2442	1844	958	484
Torque Constant (oz.-in/Amp)	.55	.73	1.41	2.79
Armature Inductance (mH)	.04	.08	.3	1.1
Back EMF Constant (mV/RPM)	.410	.542	1.04	2.067
Stall Torque (oz.-in.)[1]	1.11	1.20	1.25	1.20

Mechanical Specifications:

Mechanical Time Constant (mS)[1]	9	9	9	9
Armature Inertia (x10⁻⁴ oz-in-Sec²)	.091	.096	.096	.092
Radial Acceleration (x10³ Rad/Sec²)[1]	126	127	132	133

Bearing Play (measured at Bearing)
Radial   Less than .03 mm (.0012")
Axial   Less than .2 mm (.0079")

Thermal Resistances (°C/W)				
Rotor to Case	8	8	8	8
Case to Ambient	40	40	40	40

Max. Shaft Loading (oz)
Radial (@ 3,000 RPM)   3.60 All Types
Axial (Standing Still)   36.0 All Types
Weight (oz)   .71 All Types
Rotor Temperature Range   −30°C to +100°C

(1) Specified at Nominal Supply Voltage.
(2) Specified with Shaft Diameter = 1.5 mm. At No-Load Speed.
(3) Direction of Rotation is Reversible and Clockwise as seen from Shaft End if Red Lead or Solder Tab Marked + is
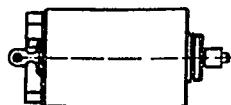   Connected to Positive Side of Voltage Supply.
                    —Specifications Subject to Change—

MOTORS

MicroMo° MOTORS

DC MicroMotors Series 1219

- Diameter 12 mm, Length 19 mm.
- Fits Screw-On Gearhead Series 10/1, and 12/3 High Torque
  (Ratios from 9:1 to 154,368:1)
- Available in 4.5, 6, 12 and 15 Volt Types.

Continuous Duty Ratings:[1]

Speeds up to 12,000 RPM

Torque up to .11 oz-in

Output Power up to .45 Watts

Electrical Specifications:

@ 72°F (22° C)

For Motor Type 1219	4.5G	006G	012G	015G
Supply Voltage nom. (Volts)	4.5	6	12	15
Armature Resistance (Ohm) ±12%	10.5	18.5	66	129
Max. Power Output (Watts)[2]	.48	.49	.55	.44
Max. Efficiency (%)[2]	69	73	72	70
No Load Speed (RPM) ±12[2]	14,400	14,300	15,600	15,400
No Load Current (mA) ±50%[3]	12	7	4	3
Friction Torque (@ No Load Speed) (oz-in)	.004	.004	.004	.004
Stall Torque (oz-in)[2]	.171	.175	.180	.145
Velocity Constant (RPM/Volt)	3292	2436	1329	1054
Back EMF Constant (mV/RPM)	.304	.411	.752	.949
Torque Constant (oz-in/Amp)	.411	.555	1.01	1.28
Armature Inductance (mH)	.15	.30	1.2	1.6

Mechanical Specifications:

Mechanical Time Constant (mS)[2]	17	17	17	17
Armature Inertia (x10⁻⁴ oz-in-Sec²)[2]	.02	.02	.02	.02
Radial Acceleration (x10³ Rad/Sec²)[2]	88.7	88.1	96.1	94.9

Bearing Play (measured at Bearing)
Radial   Less Than .03 mm (.0012")
Axial   Less Than .2mm (.0079")

Thermal Resistances (°C/W)
Rotor to Case   6 All Types
Case to Ambient   28 All Types
Max. Shaft Loading (oz)
Radial (@ 3,000 RPM)   1.8 All Types
Axial (Standing Still)   72 All Types
Weight (oz)   .39 All Types
Rotor Temperature Range   -30°C to +65°C / -22°F to +150°F
                                          -67°F to +257°F / -55°C to +125°C

(Special High Temperature Rotors
Available upon Request)

Direction of Rotation is Reversible and Clockwise as Seen From Shaft End if Red Lead or Solder Tab Marked + is
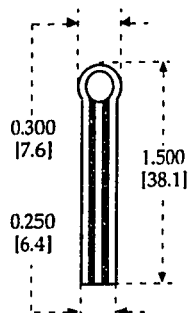Connected to Positive Side of Voltage Supply.

(1) Ratings are Presented Independent of Each Other.
(2) Specified at Nominal Supply Voltage.
(3) Specified with Shaft Diameter = .8mm. At No-Load Speed.
                              — Specifications Subject to Change —

MOTORS

B.5   The   Interlink   F.S.R:

Part #300 (1/5" Circle)

0.300
[7.6]

0.250
[6.4]

1.500
[38.1]

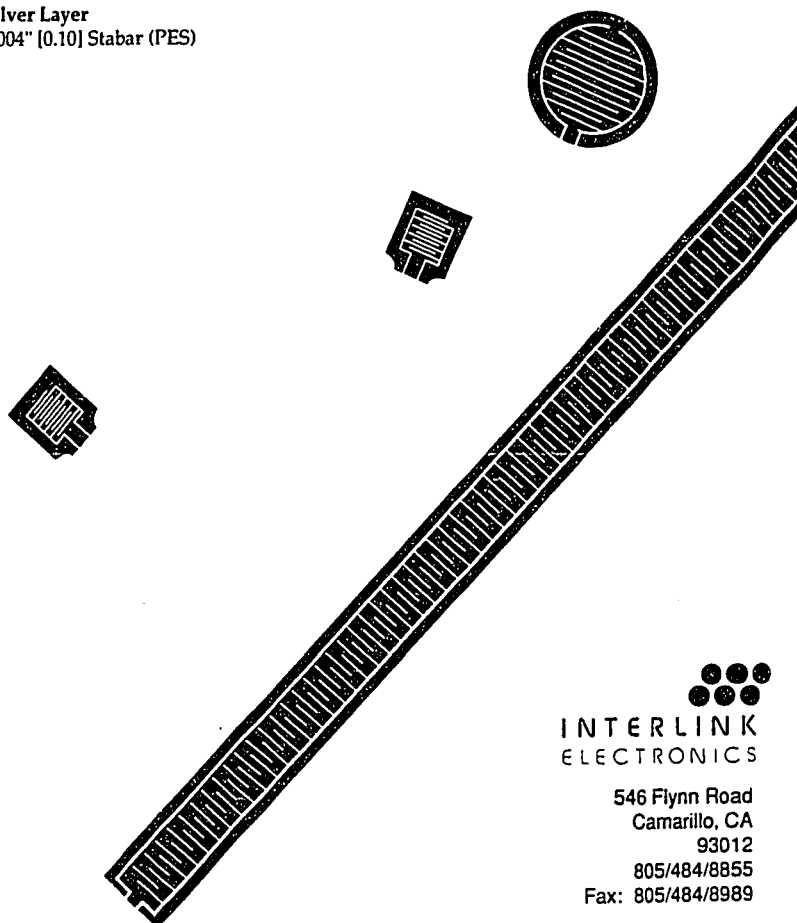**Active Area**   0.2" [5.0] diameter

Nominal Thickness   0.010" [0.25]

Material Build:

  Semiconductive Layer
  0.004" [0.10] Stabar (PES)

  Spacer Adhesive
  0.002" [0.05] Acrylic

  Silver Layer
  0.004" [0.10] Stabar (PES)

INTERLINK
ELECTRONICS

546 Flynn Road
Camarillo, CA
93012
805/484/8855
Fax: 805/484/8989

APPENDIX C: THE FRICTIONAL LOSS CALCULATION

In this appendix, we will estimate the efficiency of the power screw. Since the frictional forces dominate in this system, the forces acting on the power screw tend to oppose the motion. We follow the procedure used by Shigley and Mischke (1989) in this calculation. First imagine that a single thread of the screw is unrolled and developed (Figure C.1). Then one edge of the thread will form the hypotenuse of a right triangle whose base is the circumference of
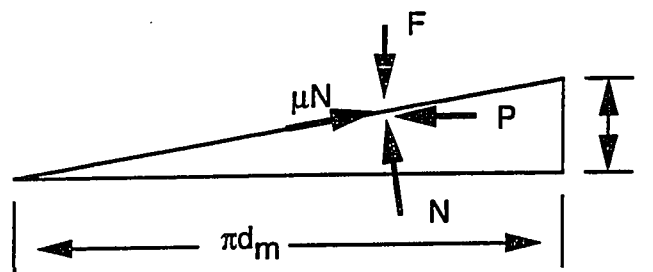

FIGURE C.1: Force diagram for the power screw

the mean-thread-diameter circle and whose height is the lead. The angle λ is the lead angle of the thread. We represent the summation of all the unit axial forces acting upon the normal thread area by F.

To move the finger, a force P acts to the right. The friction force is the product of the coefficient of friction m and the normal force N. The system is in equilibrium under the action of these forces and hence we have,

$$\sum F_H = P - N\sin(\lambda) - \mu N\cos(\lambda) = 0$$
$$\sum F_V = F + \mu N\sin(\lambda) - N\cos(\lambda) = 0$$

By eliminating N,

$$P = \frac{F(\sin(\lambda) + \mu\cos(\lambda))}{\cos(\lambda) - \mu\sin(\lambda)}$$

Dividing the numerator and the denominator by $\cos(\lambda)$ and using the relation $\tan(\lambda) = l/\pi d_m$,

$$P = \frac{F[(l/\pi d_m) + \mu]}{[1 - (\mu l/\pi d_m)]}$$

Since the torque $T = P d_m/2$

$$T = \frac{F d_m}{2}\left(\frac{1 + \pi d_m \mu}{\pi d_m - \mu l}\right)$$

Let T_0 denote the load torque without friction. Setting $\mu=0$ in the above equation,

$$T_0 = \frac{Fl}{2\pi}$$

Therefore, we get the following expression for the efficiency.

$$e = \frac{T_o}{T} = \frac{1}{d_m \pi}\left(\frac{\pi d_m - \mu l}{1 + \pi d_m \mu}\right)$$

We have assumed the coefficient of friction in our system to be 0.16. The measured values for d_m and 1 are 0.25 and 0.065 inches respectively. By substituting these quantities in to the above equation, we get the efficiency of the power screw, e to be 33.6 percent.

Reference:

[1]   Shigley, J.E. and Mischke, C.R. "Mechanical Engineering Design" McGraw-Hill Publishing Company, New York, p. 329-331, 1989.